1980

Ultimate strength of composite box girders in flexure, April 1980

Y. S. Chen

B. T. Yen

Lehigh University

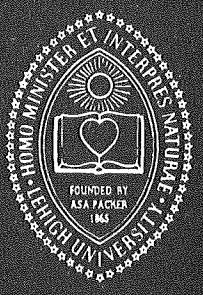

Strength of Rectangular Composite Box Girders

ULTIMATE STRENGTH OF COMPOSITE BOX GIRDERS IN FLEXURE

by
Y. S. Chen
B. T. Yen

Fritz Engineering Laboratory

Report No. 380.15 (80)

COMMONWEALTH OF PENNSYLVANIA

Department of Transportation

Office of Research and Special Studies

Istvan Januaschek, P.E. - Research Coordinator

STRENGTH OF RECTANGULAR COMPOSITE BOX GIRDERS

Project 69-4

ULTIMATE STRENGTH OF COMPOSITE BOX GIRDERS IN FLEXURE

by

Y. S. Chen

B. T. Yen

Prepared in cooperation with the Pennsylvania Department of Transportation and the U. S. Department of Transportation, Federal Highway Administration.

LEHIGH UNIVERSITY

Office of Research

Bethlehem, Pennsylvania

April 1980

Fritz Engineering Laboratory Report No. 380.15
(June 77)(80)

ABSTRACT

Ultimate strength (load carrying capacity) of rectangular steel-concrete composite box girders under flexural loading (bending and shear) without torsion is examined. Depending on the relative dimensions of the webs and the flanges, the load carrying capacity may be governed by failure of the webs, the flanges, or total plastification of the girder cross section. Interaction between bending and shear is included and both positive and negative bending moment conditions are considered. Detailed (although length) formulas are derived for different failure modes. The computed ultimate strength of two box girders compared well with test results. The procedure of this study is applicable to composite plate girder strength evaluation.

TABLE OF CONTENTS (continued)

1. INTRODUCTION

A thin-walled box girder subjected to flexural loading without torsion may be considered as equivalent to two thin-walled plate girders. The two webs of the box girder carry practically all the vertical shear and the two flanges carry most of the bending moment. The strength of the box girder is controlled by the development of the web tension field and by the strength of the flanges to resist direct compression or tension. This equivalency of box girders to plate girders has been confirmed by tests and computations[1,2,3,4]. The procedure for the ultimate strength prediction of composite box girders or composite plate girders in flexural loading, however, has not been developed and is derived in this report.

In the investigation of the ultimate strength of plate girders loaded in shear, Basler[5] proposed a uniform stress tension field model neglecting the effects of flange rigidity. The tension field in a web panel is assumed to be anchored by the neighboring web panels and the transverse stiffeners. Rockey and Skaloud[6,7,8] suggested a model which took into consideration the effects of the flange rigidity but the tension field was taken along the panel diagonal. Fujii[9,10] assumed a tension field model with the interior plastic hinges assigned at the midpanel. Chern and Ostapenko[11] developed a model consisting of two uniform stress bands and a panel mechanism.

Komatsu's model[12] assumed the flange interior plastic hinge to be independent of the extent and inclination of the tension field. More recently, Porter, Rockey and Evans[13] presented a model of single tension yield band with the position of the interior plastic hinges defined by the plastic moment capacities of the flanges. The optimal inclination of the tension field is determined by trial. This model provides identical lower and upper bound solutions, and it has been shown that many of the existing models are the special cases of this solution.

The interaction of shear and bending moment in the evaluation of load carrying capacity of thin-walled plate girders was first examined by Basler[14]. It is assumed that interaction would take place only when the external moment exceeds the flange plastic moment, the moment which can be carried by the flanges alone. Akita and Fujii[15] modified the interaction diagram of Basler's. One of the termini of the interaction diagram is determined by the shear buckling load of the web panel and the flange plastic moment. The other is defined by the ultimate shear computed by assuming no flange rigidity together with the reduced flange plastic moment computed by considering flange forces due to bending plus tension field action. Chern and Ostapenko[16] proposed a step-by-step calculation of stresses in both the tension and the compression flanges while the web is loaded into the post-buckling stage. The strength of a plate girder would be controlled by one of the following: failure of the web, buckling of the compression flange, and yielding of the tension flange.

Since consideration of the effects of flange rigidity on the tension band width is particularly important for composite girders, the model proposed by Porter, Rockey and Evans[13] together with the procedure by Chern and Ostapenko[16] for interaction between shear and bending is adopted for the strength evaluation of composite box girders.

2. GIRDERS UNDER SHEAR AND POSITIVE BENDING

A composite box girder subjected to flexural loading causing positive bending is shown in Fig. 1. A cross-section symmetrical with respect to its vertical centroidal axis may be considered as composed of two composite plate girders as depicted in Fig. 2. To account for the effects of shear lag, the equivalent flange widths computed by the procedure of Ref. 17 will be used throughout the strength evaluation.

2.1 Strength by Web Failure

The shear strength (V_u) of a panel (ABCD) of one web consists of buckling (V_{cr}) and post-buckling (V_t) contributions.

A. Buckling

The critical stresses at buckling, σ_{1c}, σ_{2c} and τ_c of Fig. 3 can be computed using the procedure of Ref. 17 in conjunction with appropriate buckling coefficients. The shear buckling force, V_{cr}, of one web can be approximated by the product of the average shearing stress, τ_c, and the area of one web, A_w.

$$V_{cr} = \tau_c A_w \tag{1}$$

B. Tension Field Action

Beyond the web buckling load, the additional vertical shear force is resisted by webs through the development of tension fields, and the corresponding additional moment is conservatively assumed to be taken by the top concrete deck and the bottom steel flange only. Three additional assumptions are made: (a) the web buckling stresses remain constant during the development of tension field and are additive with the tension field membrane stress, σ_t[5]; (b) the linearly varying normal stresses at web buckling may be idealized as uniform tensile and compressive stresses[16] as shown in Fig. 4; and (c) the ultimate strength of the panel is considered to be reached when the combination of the idealized stresses of Fig. 4 and the tension field membrane stresses, σ_t, reaches the yield condition[16].

The tension field may be divided into five sub-bands as depicted in Fig. 5. The innermost band, with width d_1, is identical to that proposed by Basler[5]. The extents of the outer bands, d_2 and d_3, depend on the rigidities of both flanges. If the flanges are rigid enough, the tension field yield zone may spread beyond the two interior plastic hinges, E and F, and form the outermost bands, d_4 and d_5, which are not contributing to the panel shear strength[13].

(a) Tension Field Shear Capacity

Let the tension field inclination angle be designated ϕ (Fig. 5), the optimal value of which is yet to be determined by maximizing the tensile membrane stress, σ_t. By expressing the idealized buckling stresses of Fig. 4 in terms of new cartesian coordinates aligned with ϕ, the resulting stresses can be combined directly with σ_t. By introducing these combined stresses in the Von Mises's yield criterion, the expression for σ_t is obtained.

$$\sigma_t = \sigma_{yw}\sqrt{\left[\frac{1}{8}\left(\frac{\sigma_{2c}}{\sigma_{yw}}\right) + \frac{3}{2}\left(\frac{r}{\sigma_{yw}}\right)\cos(2\phi - 2\delta)\right]^2 + \left[1 - 3\left(\frac{r}{\sigma_{yw}}\right)^2 - \left(\frac{\sigma_{2c}}{4\sigma_{yw}}\right)^2\right]} - \left[\frac{1}{8}\sigma_{2c} + \frac{3}{2} r \cos(2\phi - 2\delta)\right] \qquad (2a)$$

where

σ_{yw} = yield stress of the web,

$$r = \sqrt{\left(\frac{\sigma_{2c}}{4}\right)^2 + \tau_c^2} \qquad (2b)$$

and

$$\delta = \frac{1}{2}\tan^{-1}\frac{4\,|\tau_c|}{\sigma_{2c}} \qquad (2c)$$

The tension band widths d_1, d_2, and d_3 are determined by

$$d_1 = b \cos\phi - a \sin\phi \tag{3a}$$

$$d_2 = c_1 \sin\phi \tag{3b}$$

$$d_3 = c_2 \sin\phi \tag{3c}$$

where

a = panel length, may be taken to be the distance between two transverse stiffeners,

b = panel height, or the web clear height,

c_1,c_2 = distance from the corner hinge to the interior hinge of top and bottom flanges, respectively.

With the tension field band widths and intensity known, the shear capacity V_t of one web is obtained as

$$V_t = \sigma_t \, t_w b \, (\sin\phi \cos\phi - \alpha_c \sin^2\phi) \tag{4a}$$

where

t_w = web thickness,

and

$$\alpha_c = \frac{a}{b} \left(1 - \frac{c_1 + c_2}{a}\right) \tag{4b}$$

Equation 4a is identical to the ΔV_σ formula derived by Basler[5], except that the effects of flange rigidities are incorporated in the α_c term.

Because both σ_t and α_c are functions of ϕ, differentiating Eq. 4a to optimize the tension field inclination angle ϕ becomes highly complicated. However, σ_t is not sensitive to ϕ[5], and α_c does not change much with ϕ in its common range of magnitude, as can be concluded from the expressions of c_1 and c_2 to be derived later. Thus, if σ_t and α_c are treated as constants with respect to ϕ, maximization of Eq. 4a would lead to the following expression.

$$\tan\phi_{ao} = \sqrt{1 + \alpha_c^2} - \alpha_c \qquad (5)$$

where ϕ_{ao} is the approximate optimal tension field angle. The corresponding tension field shear capacity of one web is then given by

$$V_t = \frac{1}{2} \sigma_t t_w b \tan\phi_{ao} \qquad (6)$$

where σ_t computed from Eq. 2 using ϕ_{ao} from Eq. 5.

Equations 5 and 6 provide a good approximation to the tension field shear strength V_t. A procedure[18] has been developed to find the optimal tension field angle ϕ_o from ϕ_{ao} by plotting V_t against $\phi_{ao} + \Delta\phi$. The maximum value of V_t can be found accordingly.

(b) Locations of Interior Plastic Hinges

The locations of the interior plastic hinges in the flanges caused by the tension field force are determined by the flange plastic bending moment capacities, which are influenced by the presence of

axial forces in the flanges. For the equivalent rectangular bottom flange, the modified plastic moments at the corner hinge D and the interior hinge F (Fig. 5) to account for the existence of axial stresses are given as[19]

$$M_p^c = M_p \left[1 - \left(\frac{\sigma_{bf}^c}{\sigma_{bf}^y}\right)^2\right] \tag{7a}$$

$$M_p^i = M_p \left[1 - \left(\frac{\sigma_{bf}^i}{\sigma_{bf}^y}\right)^2\right] \tag{7b}$$

where

M_p^c, M_p^i = the modified plastic moments at the corner and the interior hinges, respectively, in the bottom flange in the width w_{e2} (Fig. 2),

w_{e2} = half of the equivalent width of the bottom flange plus the small projecting width beyond the web,

M_p = the full plastic moment capacity of the bottom flange in the width w_{e2},

σ_{bf}^c, σ_{bf}^i = the corresponding normal stresses at the corner and the interior plastic hinges, and,

σ_{bf}^y = the yield stress of the bottom flange.

where

$$\alpha_c' = \frac{a}{b}\left(\frac{1}{2} - \frac{c_2}{a}\right) \tag{9b}$$

(c) Normal Stresses or Forces at the Hinges

To calculate the hinge locations c_1 and c_2, the modified plastic moment capacities of the flanges at the hinges to account for the axial forces need to be evaluated. This requires that the axial forces present at the hinges be found before the computation of modified plastic moments. The axial stresses or forces at the onset of web buckling will be found first.

At the corner hinge D of the bottom flange (Fig. 1) the normal stress is:

$$\sigma_{bf}^{c1} = \frac{V_{cr}\,(L - z_1)y_{bf}}{I_x/2} \tag{10a}$$

At the interior hinge

$$\sigma_{bf}^{i1} = \frac{V_{cr}\,(L - z_1 - c_2)y_{bf}}{I_x/2} \tag{10b}$$

where

V_{cr} = shear buckling strength of the panel of one web in question,

z_1 = distance from the left support to the left boundary of the panel,

y_{bf} = distance from the mid-thickness of bottom flange to the centroid of the equivalent box girder cross-section (Fig. 2) and,

I_x = moment of inertia about the horizontal, centroidal (x) axis of the same equivalent box girder cross-section.

For the compression flange cross-section consisting of concrete deck and top steel flanges, the longitudinal strain through the thickness is assumed as uniform, thus the total axial force in the combined section is acting at the elastic centroid. The location of the elastic centroid (Fig. 2) is given as

$$\bar{t}_{ec} = \frac{0.5\, A_g\, (t_c + t_{tf}) + (n - 1)\, A_{s1}(t_c - t_1 + 0.5\, t_{tf})}{A_t} + \frac{(n - 1)\, A_{s2}\, (t_2 + 0.5 t_{tf})}{A_t} \qquad (11)$$

where

$\bar{t}_{ec}$ = distance from the mid-thickness of the top steel flange to the elastic centroid of the combined compression flange cross-section,

A_g = $t_c \cdot w_{el}$, the gross concrete area in the width w_{el},

w_{el} = half of the equivalent width of the concrete deck,

t_c = thickness of the concrete deck,

t_{tf} = thickness of the top steel flange,

A_{tf} = cross-sectional area of the top steel flange,

n = E_s/E_c, the modular ratio,

E_s = the elastic modulus of steel, taken to be 203,550 MN/m^2 (29,500 ksi) for both reinforcing bars and steel component plates,

E_c = the elastic modulus of concrete,

A_{s1} = total area of longitudinal reinforcement of top layer in the width w_{el},

A_{s2} = total area of longitudinal reinforcement of bottom layer in w_{el},

t_1 = the distance from the center of top longitudinal reinforcing bars to the top fiber of concrete deck,

t_2 = the distance from the center of bottom longitudinal reinforcing bars to the bottom fiber of concrete deck, and

A_t = $nA_{tf} + A_g + (n - 1)(A_{s1} + A_{s2})$, the transformed area of the combined section in the width w_{el}.

At the corner hinge B the axial force in the combined section of the width w_{el} is given by

$$F_{cf}^{c1} = \frac{V_{cr}(L - z_1 - a)(y_{tf} + \bar{t}_{ec})}{I_x/2} \cdot \frac{A_t}{n} \qquad (12a)$$

At the interior hinge E, it is

$$F_{cf}^{il} = \frac{V_{cr}(L - z_1 - a + c_1)(y_{tf} + \bar{t}_{ec})}{I_x/2} \cdot \frac{A_t}{n} \qquad (12b)$$

If the concrete deck is handled as an elastic plane stress orthotropic plate as suggested in Ref. 17, then the longitudinal elastic modulus E_z has to be used, and Eqs. 11 and 12 revised accordingly for calculating the axial force at the hinges at web buckling.

In addition to the stresses and forces, σ_{bf}^{il}, σ_{bf}^{cl}, F_{cf}^{il} and F_{cf}^{cl}, developed at the onset of web buckling, there are forces induced by the horizontal component of the tension field stresses as well as by the external moment necessary for equilibrium with the tension field shear V_t.

The horizontal component of the tension field force in the innermost (Basler) band d_1 (Fig. 6) is computed by

$$H_{tB} = \sigma_t \, t_w b(\cos^2\phi - \frac{a}{b} \sin\phi \cos\phi) \qquad (13)$$

It is assumed that half of this horizontal component is carried in compression by the bottom flange and the at the two corner hinges, D and B, respectively. That is

$$H_{bf}^{c} = H_{tf}^{c} = H_{tB}/2 \qquad (14)$$

where

H_{bf}^{c} = the horizontal normal force, induced by the tension field action, acting at the mid-thickness of the bottom flange, and

H_{tf}^{c} = the similar horizontal normal force acting at the mid-thickness of the top steel flange.

It is to be noted that the tension field inclination angle may be such that the H_{tB} value is negative. If this occurs, it is assumed that no horizontal component of the tension field stresses is taken by the two corner hinges. Thus, $H_{bf}^{c} = H_{tf}^{c} = 0$.

At the interior hinges, F and E, where the horizontal components of bands d_2 and d_3 act, the total horizontal normal forces are

$$H_{bf}^{i} = H_{bf}^{c} + \sigma_t \, t_w \, c_2 \sin\phi \cos\phi \qquad (15a)$$

$$H_{tf}^{i} = H_{tf}^{c} + \sigma_t \, t_w \, c_1 \sin\phi \cos\phi \qquad (15b)$$

which are acting at the mid-thickness of the respective flange.

The normal forces created by the external moment equilibrium are designated as F_{bf}^{c2} and F_{bf}^{i2}, and F_{cf}^{c2} and F_{cf}^{i2} for the corner and interior hinges of the bottom and top combined flanges, respectively. The location of F_{bf}^{c2} and F_{bf}^{i2} is naturally at the

mid-thickness of the bottom flange, whereas that of F_{cf}^{c2} and F_{cf}^{i2} is assumed to be at the plastic centroid of the combined section of the concrete deck and top steel flanges. The plastic centroid of the combined section in the equivalent width w_{el} is shown in Fig. 7 and is computed by[20]

$$\bar{t}_{pc} = [0.425\ f_c'\ A_g\ (t_c + t_{tf}) + (\sigma_{s1}^y - 0.85\ f_c')\ A_{s1}\ (t_c - t_1 + 0.5\ t_{tf}) + (\sigma_{s2}^y - 0.85\ f_c')\ A_{s2}\ (t_2 + 0.5\ t_{tf})]/F_{cf}^u \tag{16a}$$

where

$\bar{t}_{pc}$ = distance from the mid-thickness of top steel flange to the plastic centroid, and

F_{cf}^u = the ultimate concentric load of the combined section in w_{el}.

The force F_{cf}^u is given by

$$F_{cf}^u = 0.85\ f_c'\ A_g + \sigma_{tf}^y\ A_{tf} + (\sigma_{s1}^y - 0.85\ f_c')\ A_{s1} + (\sigma_{s2}^y - 0.85\ f_c')\ A_{s2} \tag{16b}$$

in which σ_{tf}^y, σ_{s1}^y, and σ_{s2}^y are respectively the yield stress of A_{tf}, A_{s1}, and A_{s2}. Once $\bar{t}_{pc}$ is determined, the forces are computed (Figs. 1 and 2) by

$$F_{bf}^{c2} = \frac{V_t\ (L - z_1)}{b' + \bar{t}_{pc}} \tag{17a}$$

$$F_{bf}^{i2} = \frac{V_t\ (L - z_1 - c_2)}{b' + \bar{t}_{pc}} \tag{17b}$$

$$F_{cf}^{c2} = \frac{V_t\ (L - z_1 - a)}{b' + \bar{t}_{pc}} \tag{17c}$$

$$F_{cf}^{i2} = \frac{V_t\ (L - z_1 - a + c_1)}{b' + \bar{t}_{pc}} \tag{17d}$$

where b' is the distance from the mid-thickness of bottom flange to that of top steel flange.

The total normal stress, including buckling and post-buckling stages, in the bottom flange at the corner hinge D is

$$\sigma_{bf}^{c} = \sigma_{bf}^{c1} + \frac{F_{bf}^{c2} - H_{bf}^{c}}{A_{bf}} \tag{18a}$$

and that at the interior hinge F is

$$\sigma_{bf}^{i} = \sigma_{bf}^{i1} + \frac{F_{bf}^{i2} - H_{bf}^{i}}{A_{bf}} \tag{18b}$$

where

$A_{bf} = t_{bf}\ w_{e2}$, the bottom flange area in the equivalent width, w_{e2},

t_{bf} = thickness of the bottom flange.

By substituting Eqs. 18 into Eqs. 7, the modified plastic moments at the hinges of the bottom flange can be found.

(d) Ultimate Moment Capacities at the Hinges of Top Flange

In evaluating the ultimate moment capacities at the hinges of the compression flange, general assumptions used in the reinforced concrete design are followed. The maximum usable strain at the extreme concrete compressive fiber, ε_{cu}, is taken to be 0.003, and the rectangular equivalent stress block is used[21]. The stress-strain relationship of the reinforcing bars and top steel flange is idealized as elastic-perfectly-plastic as shown in Fig. 8.

The interior hinge E is treated first. Figure 7 depicts the strain and force diagrams of the hinge. From the strain diagram it is deduced

$$k_u = \frac{0.003}{\varepsilon_{tf} + 0.003} \tag{19}$$

where

k_u = a coefficient for determining the neutral axis, and

ε_{tf} = the strain at the mid-thickness of the top steel flange.

The forces in the equivalent deck width of w_{el} are computed as follows:

By the equilibrium of the plastic moments and the vertical components of the tension field stresses in the segment $\overline{DF}$ shown in Fig. 6 the interior hinge location, c_2, can be computed.

$$c_2 = \sqrt{\frac{2(M_p^{\,c} + M_p^{\,i})}{\sigma_t\, t_w \sin^2\phi}} \leq a \qquad (8a)$$

For the compression flange, which has the combined section of the concrete deck and two top steel flanges, the modified ultimate moment capacities have to be found by trial, and will be discussed later. The location of the interior hinge, c_1, can be computed in the same manner as for c_2.

$$c_1 = \sqrt{\frac{2(M_u^{\,c} + M_u^{\,i})}{\sigma_t\, t_w \sin^2\phi}} \leq a \qquad (8b)$$

where $M_u^{\,c}$ and $M_u^{\,i}$ are the ultimate moments at the corner and the interior hinges, respectively. Both c_1 and c_2 are limited by the panel length a. If both are equal to a, the web panel boundary frame will form a panel mechanism as suggested in Ref. 16. If the computed values of c_1 and c_2 from Eqs. 8 are such that $c_1 \geq a$ and $c_2 \geq a$, a case often occurs to composite box girders, then Eqs. 4 become

$$V_t = \sigma_t\, t_w b\, (\sin\phi \cos\phi - \alpha_c' \sin^2\phi) + \frac{M_u^{\,c} + M_u^{\,i}}{a} \qquad (9a)$$

$$C_{s1} = (\sigma_{s1} - 0.85\, f_c')\, A_{s1} \qquad (20a) \quad (20a)$$

$$C_c = 0.85\, f_c'\, \beta_1\, k_u t_3\, w_{el} \qquad (20b) \quad (20b)$$

$$T_{s2} = \sigma_{s2}\, A_{s2} \qquad (20c) \quad (20c)$$

$$T_{tf} = \sigma_{tf}\, A_{tf} \qquad (20d) \quad (20d)$$

where

C_{s1} = the total compressive force in the reinforcing bar area A_{s1} minus the corresponding concrete force in the same area,

σ_{s1} = the stress in the bar area A_{s1},

C_c = the total concrete force in the equivalent rectangular stress block,

f_c' = concrete strength,

β_1 = a fraction taken as 0.85 for concrete strength f_c' up to 27.6 MN/m^2 (4 ksi), and reduced continuously at a rate of 0.05 for each 6.9 MN/m^2 (1 ksi) of strength in excess of 27.6 MN/m^2 (4 ksi)[21],

t_3 = $t_c + 0.5\, t_{tf}$ (Fig. 7),

T_{s2} = total tensile force in the bar area A_{s2},

σ_{s2} = the stress in the bar area A_{s2},

T_{tf} = total tensile force in one top steel flange, A_{tf}, and

σ_{tf} = the stress in A_{tf}.

The equilibrium of the horizontal forces gives rise to

$$\sigma_{tf} = \frac{0.00255\, f_c' \beta_1}{\varepsilon_{tf} + 0.003} \cdot \frac{t_3\, w_{el}}{A_{tf}} + (\sigma_{s1} - 0.85\, f_c') \frac{A_{s1}}{A_{tf}} - \sigma_{s2} \frac{A_{s2}}{A_{tf}} - \frac{F_{cf}^{i1} + F_{cf}^{i2} + H_{tf}^{i}}{A_{tf}} \qquad (21)$$

The neutral axis can be located by trial using Eq. 21. Because at ultimate moment the A_{s1} bars are most likely at yielding, $\sigma_{s1} = \sigma_{s1}^{y}$ can first be assumed. An appropriate value of the stress in A_{s2} bars is then assumed by judgment according to the top steel flange area A_{tf}. From the idealized stress-strain relationship of A_{tf} its stress and strain (σ_{tf} and ε_{tf}) can be determined. The value of k_u is then computed from Eq. 19. The strains ε_{s1} and ε_{s2} can be obtained from the strain diagram and the corresponding stresses σ_{s1} and σ_{s2} determined from their individual stress-strain relationship. This process can be repeated until the assumed and computed values of σ_{s1} and σ_{s2} agree satisfactorily.

With the neutral axis located, the forces as defined in Eqs. 20 can be determined. The ultimate moment capacity M_u^i at the interior hinge E of the compression flange in the equivalent width w_{el} (Fig. 7) is computed by

$$M_u^i = C_{s1}\,(k_u\,t_3 - t_1) + C_c(1 - 0.5\,\beta_1)\,k_u\,t_3 + T_{s2}\,(t_c - t_2 - k_u t_3) + (T_{tf} + H_{tf}^i)(1 - k_u)t_3 + F_{cf}^{i1}\,[(1 - k_u)t_3 - \bar{t}_{ec}] + F_{cf}^{i2}\,[(1 - k_u)t_3 - \bar{t}_{pc}] \qquad (22)$$

The ultimate moment at the corner hinge B bends the compression flange concave-downward. The moment capacity is reached when the tensile reinforcing bars A_{s1} attain the rupture strain or the concrete compressive strain at the bottom fiber arrives at its crushing value of 0.003. These cases are treated separately below.

When the tensile reinforcing bars A_{s1} rupture, the compressive strain of the top steel flange may be less than the yield strain and the corresponding bottom fiber strain of the concrete deck less than the idealized yielding value (Fig. 7)($\varepsilon_{s1} = \varepsilon_{s1}^u$, $\varepsilon_{tf} < \varepsilon_{tf}$, $\varepsilon_c \leq \varepsilon_{cy}$). From the strain diagram in Fig. 8a, it is deduced

$$k_u = 1 - \frac{\varepsilon_{s1}^u}{\varepsilon_{tf} + \varepsilon_{s1}^u} \qquad (23)$$

The forces in the equivalent width w_{el} are:

$$T_{s1} = \sigma_{s1}^{y} A_{s1} \tag{24a}$$

$$C_c = 0.5\ f_c\ (k_u\ t_4 - 0.5\ t_{tf})\ w_{el} \tag{24b}$$

$$C_{s2} \doteqdot (\sigma_{s2} - f_c)\ A_{s2},\ \text{for } k_u t_4 > 0.5\ t_{tf} + t_2 \tag{24c}$$

$$C_{tf} = \sigma_{tf}\ A_{tf} \tag{24d}$$

where

T_{s1} = the total tensile force in the bars A_{s1},

C_c = the concrete force in the elastic, triangular stress block,

f_c = concrete stress at extreme compressive fiber,

$t_4 = t_c - t_1 + 0.5\ t_{tf}$,

C_{s2} = total compressive force in the bars A_{s2} minus the corresponding concrete force in the same area, with the concrete stress conservatively taken as f_c, and

C_{tf} = total compressive force in one top steel flange of area A_{tf}.

The equilibrium of horizontal forces results in

$$\sigma_{tf} = 0.5\ f_c \frac{\epsilon_{s1}^u}{\epsilon_{tf} + \epsilon_{s1}^u} \cdot \frac{t_4\ w_{el}}{A_{tf}} - 0.5\ f_c \frac{(t_4 - 0.5\ t_{tf})\ w_{el}}{A_{tf}} + \sigma_{s1}^y \frac{A_{s1}}{A_{tf}} - (\sigma_{s2} - f_c) \frac{A_{s2}}{A_{tf}} + \frac{F_{cf}^{c1} + F_{cf}^{c2} + H_{tf}^c}{A_{tf}} \tag{25}$$

Equation 25 can be used for locating the neutral axis by trial. Appropriate values of f_c and σ_{s2} are first assumed. The values of σ_{tf} and ϵ_{tf} are then determined through the idealized $\sigma_{tf} - \epsilon_{tf}$ relationship. The neutral axis can be located by Eq. 23 and the strains ϵ_c and ϵ_{c2} obtained. The corresponding stresses f_c and σ_{s2} can be re-evaluated through the idealized stress-strain relationships. The procedure is repeated until the assumed stresses agree satisfactorily with those computed. After the neutral axis and the horizontal forces are determined, the ultimate moment capacity at hinge B in the equivalent width w_{el} can be computed by

$$M_u^c = T_{s1}(1 - k_u)t_4 + \frac{2}{3} C_c(k_u t_4 - 0.5\ t_{tf})$$

$$+ C_{s2}(k_u t_4 - 0.5\ t_{tf} - t_2) + (C_{tf} - H_{tf}^c)\ k_u t_4$$

$$+ F_{cf}^{c1}\ (\bar{t}_{ec} - k_u t_4) + F_{cf}^{c2}\ (\bar{t}_{pc} - k_u t_4) \qquad (26)$$

It is to be noted that if $k_u t_4 < 0.5\ t_{tf} + t_2$, then A_{s2} is in tension. The f_c term in both Eqs. 24c and 25 has to be dropped and the sign of σ_{s2} changed to negative. However, Eq. 26 is still valid.

When the tensile reinforcing bars A_{s1} rupture, the top steel flange may remain elastic, and the concrete bottom fiber may have exceeded the idealized yield but not reached the crushing strain. The force diagram of this case is shown in Fig. 9b. Since ϵ_c has not reached its crushing value, a trapezoidal stress block is used. In Fig. 9b, t_5 defines the distance from the neutral axis to the concrete fiber where the strain is equal to ϵ_{cy}. Equation 23 remains applicable. The forces in the concrete and the reinforcing bars are:

$$C_{c1} = f_c'\ (k_u t_4 - 0.5\ t_{tf} - t_5)\ w_{el} \qquad (27a)$$

$$C_{c2} = 0.5\ f_c'\ t_5\ w_{el} \qquad (27b)$$

$$C_{s2} = (\sigma_{s2} - f_c')\ A_{s2} \qquad (27c)$$

$$t_5 = \frac{\epsilon_{cy}}{\epsilon_{tf} + \epsilon_{s1}^u} t_4 \qquad (27d)$$

$$T_{s1} = \sigma_{s1}^{y} A_{s1} \tag{27e}$$

$$C_{tf} = \sigma_{tf} A_{tf} \tag{27f}$$

where

C_{c1} = total concrete force corresponding to the block of uniform stress f_c',

C_{c2} = total concrete force in the stress triangle of Fig. 8b corresponding to the distance t_5, and

C_{s2} = total compressive force in A_{s2} minus the corresponding concrete force in the same area; if the concrete stress at the A_{s2} level is smaller than f_c', it will be conservatively taken as f_c'.

Equations 27e and 27f are identical to Eqs. 24a and 24d, respectively. The equilibrium of the horizontal forces gives the expression for σ_{tf}.

$$\sigma_{tf} = f_c' \frac{\epsilon_{s1}^{u} + 0.5\,\epsilon_{cy}}{\epsilon_{tf} + \epsilon_{s1}^{u}} \cdot \frac{t_4\, w_{el}}{A_{tf}} - f_c' \frac{(t_4 - 0.5\, t_{tf}) w_{el}}{A_{tf}}$$

$$+ \sigma_{s1}^{y} \frac{A_{s1}}{A_{tf}} - (\sigma_{s2} - f_c') \frac{A_{s2}}{A_{tf}}$$

$$+ \frac{F_{cf}^{c1} + F_{cf}^{c2} + H_{tf}^{c}}{A_{tf}} \tag{28}$$

Again, the neutral axis can be located by trial. In this case only the stress σ_{s2} needs to be assumed. After the forces are calculated, the ultimate moment capacity is computed by

$$M_u^c = T_{s1}\,(1 - k_u)t_4 + 0.5\,C_{c1}\,(k_u t_4 - 0.5\,t_{tf} + t_5)$$

$$+ \frac{2}{3}\,C_{c2}\,t_5 + C_{s2}\,(k_u t_4 - 0.5\,t_{tf} - t_2)$$

$$+ (C_{tf} - H_{tf}^c)k_u t_4 + F_{cf}^{c1}\,(\bar{t}_{ec} - k_u t_4)$$

$$+ F_{cf}^{c2}(\bar{t}_{pc} - k_u t_4) \qquad (29)$$

If the top steel flange A_{tf} is relatively small, the plastic hinge B may be formed because of the crushing of the concrete (Fig. 9c). By the same procedure as employed previously, the following equations are arrived:

$$k_u = \frac{0.003}{\varepsilon_{s1} + 0.003} \qquad (30)$$

$$T_{s1} = \sigma_{s1}\,A_{s1} \qquad (31a)$$

$$C_c = 0.85\,f_c'\,\beta_1\,k_u t_6\,w_{el} \qquad (31b)$$

$$C_{s2} = (\sigma_{s2} - 0.85\,f_c')\,A_{s2} \qquad (31c)$$

$$C_{tf} = \sigma_{tf}^y\,A_{tf} \qquad (31d)$$

where $t_6 = t_c - t_1$, the distance from A_{s1} to concrete extreme compressive fiber. The expression for the stress in bars A_{s1} is:

$$\sigma_{s1} = \frac{0.00255\, f_c' \beta_1}{\epsilon_{s1} + 0.003} \cdot \frac{t_6\, w_{el}}{A_{s1}} + (\sigma_{s2} - 0.85\, f_c') \frac{A_{s2}}{A_{s1}} + \sigma_{tf}^{y} \frac{A_{tf}}{A_{s1}} - \frac{F_{cf}^{c1} + F_{cf}^{c2} + H_{tf}^{c}}{A_{s1}} \qquad (32)$$

When locating the neutral axis by trial using Eq. 32, only the stress σ_{s2} needs to be assumed for the first trial. The ultimate moment capacity at hinge B is

$$M_u^c = T_{s1}(1 - k_u)t_6 + C_c(1 - 0.5\,\beta_1)k_u t_6 + C_{s2}(k_u t_6 - t_2) + (C_{tf} - H_{tf}^{c})(k_u t_6 + 0.5\, t_{tf}) + F_{cf}^{c1}(\bar{t}_{ec} - k_u t_6) + F_{cf}^{c2}(\bar{t}_{pc} - k_u t_6) \qquad (33)$$

(e) Determination of Interior Hinge Locations

Since the magnitudes of M_p^c, M_p^i, M_u^c and M_u^i all depend upon the hinge locations c_1 and c_2, which in turn are functions of these ultimate moments, the determination of c_1 and c_2 must be conducted by iteration. The following process is suggested:

(1) Assume $c_1 = c_2 = a/2$.

(2) Compute σ_{bf}^{c1}, σ_{bf}^{i1}, H_{bf}^{c} and H_{bf}^{i} with σ_t from Eqs. 2 and 5; and F_{bf}^{c2} and F_{bf}^{i2}, with V_t from Eq. 6. Compute M_p^c and M_p^i.

(3) In a way similar to step (2), compute F_{cf}^{c1}, F_{cf}^{i1}, H_{tf}^{c}, F_{cf}^{c2} and F_{cf}^{i2}. Compute M_u^i by Eq. 22, and M_u^c by Eq. 26, 29 or 33, whichever is applicable.

(4) Compute c_2 and c_1 by Eqs. 8.

(5) Repeat steps 2 through 4 until satisfactorily steady values of c_1 and c_2 are obtained.

(6) Compute optimal angle ϕ_o and the associated σ_t and V_t by Eqs. 4 or 9. Repeat steps 2, 3 and 4 using the optimal values of σ_t and V_t until satisfactorily steady values of c_1 and c_2 are obtained.

By using the values of c_1 and c_2 obtained from step 6, the tension field shear capacity of the panel of one web, V_t, is determined.

The ultimate shear capacity of the panel of one web is the sum of the buckling and post-buckling contributions.

$$V_u = V_{cr} + V_t \tag{34}$$

The ultimate load P_u, which causes failure of the panel of two webs of the box girder (Fig. 1), is computed by

$$P_u = \frac{2\ V_u}{\alpha} \tag{35}$$

where α is a factor defining the location of the load.

2.2 Strength by Flange Failure

A box girder panel, subjected to bending moment and shear without external load on the panel, has a bending moment higher at one end than that at the other. The bottom flange may yield or the concrete deck may crush at the end of the higher moment before full development of the tension field.

At the web panel buckling, normal stress and force in the steel bottom flange and in the composite top flange are, respectively,

$$\sigma_{bf}^{cr} = \frac{V_{cr}\,(L - z_1)\,y_{bf}}{I_x/2} \tag{36a}$$

$$F_{cf}^{cr} = \frac{V_{cr}\,(L - z_1)(y_{tf} + \bar{t}_{pc})}{I_x/2} \cdot \frac{A_t}{n} \tag{36b}$$

For simplicity, F_{cf}^{cr} is computed at the plastic centroid instead of at the elastic centroid. The additional tensile force needed to cause yielding of the bottom flange in the width w_{e2} is

$$\Delta F_{bf} = (\sigma_{bf}^{y} - \sigma_{bf}^{cr})\,A_{bf} \tag{37a}$$

and the additional compressive force needed to cause failure of the combined compression flange section (w_{e1}) is

$$\Delta F_{cf} = F_{cf}^{u} - F_{cf}^{cr} \tag{37b}$$

where F_{cf}^{u} is from Eq. 16b. If the smaller of ΔF_{bf} and Δ_{cf} is denoted as ΔF which controls the strength, then the shear strength corresponding to the failure of the flange is

$$V_f = \frac{\Delta F\,(b' + \bar{t}_{pc})}{L - z_1} \tag{38}$$

Equation 38 is conservative in that the capacity of the web in resisting bending after buckling has been neglected. However, it is unconservative in that the normal force in the concrete deck due to incomplete tension field have been also neglected. These effects are assumed to compensate each other. The ultimate shear capacity of one web is the sum of the buckling strength and V_f.

$$V_u = V_{cr} + V_f \tag{39}$$

The ultimate load, P_u, can be computed by Eq. 35.

For most composite box girders the neutral axis is close to the concrete deck, thus yielding of the bottom flange occurs prior to failure of the compression flange. Because most of the structural steels have good ductility and are capable of strain hardening, unless the bottom flange plate is very thin, the final failure of composite box girders in bending would most likely be by crushing of the concrete deck with bottom flange stresses in the strain hardening range. In this case, the ΔF_{bf} value computed using σ_{bf}^{u}, the ultimate tensile strength of the bottom flange plate, in place of the σ_{bf}^{y} term in Eq. 37a would be larger than the ΔF_{cf} from Eq. 37b. Thus the latter would be used as ΔF in Eq. 38 for strength computation.

2.3 Strength by Full Plastification of the Cross Section

If a web panel does not buckle prior to the yielding of the bottom flange within that panel, the yielding may penetrate into the webs and result in full plastification of the cross section. Let τ and σ be the average shear and the normal stress at the general

yielding of the web, as shown in Fig. 10, then the ultimate shear capacity of one web is

$$V_u = \tau A_w \tag{40}$$

and from the von Mises's yield condition,

$$\left(\frac{V_u}{V_p}\right)^2 + \left(\frac{\sigma}{\sigma_{yw}}\right)^2 = 1 \tag{41}$$

where $V_p = \sigma_{yw} A_w/\sqrt{3}$ is the plastic shear of the web.

Figure 10 depicts two cases of plastification: one with neutral axis in the webs and the other in the concrete deck. For the case where the neutral axis is in the webs, Fig. 10a, the forces in half of the equivalent cross section are computed by

$$C_c = 0.85 f_c' A_g \tag{42a}$$

$$C_{s1} = (\sigma_{s1}^y - 0.85 f_c') A_{s1} \tag{42b}$$

$$C_{s2} = (\sigma_{s2}^y - 0.85 f_c') A_{s2} \tag{42c}$$

$$C_{tf} = \sigma_{tf}^y A_{tf} \tag{42d}$$

$$C_w = \sigma t_w (k_u d - t_c - t_{tf}) \tag{42e}$$

$$T_w = \sigma t_w [(1 - k_u) d - 0.5 t_{bf}] \tag{42f}$$

$$T_{bf} = \sigma_{bf}^y A_{bf} \tag{42g}$$

where

C_w, T_w = the compressive and tensile force in the web portion above and below the neutral axis, respectively,

$d = t_c + t_{tf} + b + 0.5 t_{bf}$, and

T_{bf} = the tensile force in the bottom flange in the width w_{e2}.

The condition of equilibrium of horizontal forces enables the evaluation of the coefficient k_u for determining the neutral axis.

$$k_u = k_1 - \frac{s_1}{\sigma} \tag{43a}$$

where

$$k_1 = \frac{1}{2d} (d + t_c + t_{tf} - 0.5\ t_{bf}) \tag{43b}$$

$$s_1 = \frac{1}{2d\ t_w} (C_c + C_{s1} + C_{s2} + C_{tf} - T_{bf}) \tag{43c}$$

The ultimate moment of half of the equivalent box girder cross section is given as

$$M_u = (v_1 + v_2)\ \sigma - \frac{s_1\ m_5}{\sigma} + m_6 \tag{44a}$$

where

$$v_1 = \frac{1}{2}\ t_w\ (k_1\ d - t_c - t_{tf})^2 \tag{44b}$$

$$v_2 = \frac{1}{2}\ t_w\ [(1 - k_1)\ d - 0.5\ t_{bf}]^2 \tag{44c}$$

$$m_5 = s_1\ t_w\ d^2 \tag{44d}$$

$$m_6 = m_1 - m_2 - m_3 + m_4 \tag{44e}$$

$$\begin{aligned} m_1 = {} & C_c\ (k_1\ d - 0.5\ t_c) + C_{s1}\ (k_1\ d - t_1) \\ & + C_{s2}\ (k_1\ d - t_c + t_2) + C_{tf}\ (k_1\ d \\ & - t_c - 0.5\ t_{tf}) + T_{bf}\ (1 - k_1)d \end{aligned} \tag{44f}$$

$$m_2 = \frac{1}{2}\ s_1\ t_w\ d\ [(1 - 2k_1)d + t_c + t_{tf} - 0.5\ t_{bf}] \tag{44g}$$

$$m_3 = \frac{1}{2}\ s_1\ t_w\ d\ (k_1\ d - t_c - t_{tf}) \tag{44h}$$

$$m_4 = \frac{1}{2}\ s_1\ t_w\ d\ [(1 - k_1)d - 0.5\ t_{bf}] \tag{44i}$$

By the equilibrium of internal and external moments at the panel boundary $z = z_1$ (Fig. 1), it is derived

$$\frac{V_u}{V_p} = \frac{1}{V_p\,(L - z_1)} \left[(v_1 + v_2)\,\sigma_{yw}\,\left(\frac{\sigma}{\sigma_{yw}}\right) - \frac{s_1\,m_5}{\sigma_{yw}}\left(\frac{\sigma_{yw}}{\sigma}\right) + m_6\right] \tag{45}$$

Equation 45 in conjunction with the interaction equation, Eq. 41, can be used to solve for V_u and σ graphically. With V_u/V_p as the ordinate and σ/σ_{yw} the abscissa, the intersecting point of the two curves gives the solution values of V_u/V_p and σ/σ_{yw}. After V_u is determined, the ultimate load P_u can be computed by Eq 35.

For the case where the neutral axis is in the concrete deck (Fig. 10b), the forces are

$$C_c = 0.85\,f_c'\,\beta_1\,k_u\,d\,w_{el} \tag{46a}$$

$$C_{s1} = (\sigma_{s1}^y - 0.85\,f_c')\,A_{s1} \tag{46b}$$

$$T_{s2} = \sigma_{s2}^y\,A_{s2} \tag{46c}$$

$$T_{tf} = \sigma_{tf}^y\,A_{tf} \tag{46d}$$

$$T_w = \sigma\,A_w \tag{46e}$$

$$T_{bf} = \sigma_{bf}^y\,A_{bf} \tag{46f}$$

By the same procedure as employed previously, the following equations are arrived:

$$k_u = k_2\,\frac{\sigma}{f_c'} + k_3 \tag{47a}$$

where

$$k_2 = \frac{A_w}{0.85\ \beta_1\ d\ w_{el}} \tag{47b}$$

$$k_3 = \frac{T_{s2} + T_{tf} + T_{bf} - C_{s1}}{0.85\ f_c'\ \beta_1\ d\ w_{el}} \tag{47c}$$

$$M_u = \frac{v_3}{f_c'}\sigma^2 + (v_4 + v_5 + \frac{m_7}{f_c'})\ \sigma + m_8 \tag{48a}$$

where

$$v_3 = -0.5\ \beta_1\ k_2\ d\ A_w \tag{48b}$$

$$v_4 = -0.5\ \beta_1\ k_3\ d\ A_w \tag{48c}$$

$$v_5 = A_w\ (d - 0.5\ t_{bf} - 0.5\ b) \tag{48d}$$

$$m_7 = -0.5\ \beta_1\ k_2\ d(T_{s2} + T_{tf} + T_{bf} - C_{s1}) \tag{48e}$$

$$m_8 = -0.5\ \beta_1\ k_3\ d(T_{s2} + T_{tf} + T_{bf} - C_{s1}) - C_{s1}\ t_1 + T_{s2}\ (t_c - t_2) + T_{tf}\ (d - 0.5\ t_{bf} - b - 0.5\ t_{tf}) + T_{bf}\ d \tag{48f}$$

$$\frac{V_u}{V_p} = \frac{1}{V_p(L - z_1)}\left[\frac{v_3\ \sigma_{yw}^2}{f_c'}\left(\frac{\sigma}{\sigma_{yw}}\right)^2 + (v_4 + v_5 + \frac{m_7}{f_c'})\ \sigma_{yw}\ (\frac{\sigma}{\sigma_{yw}}) + m_8\right] \tag{49}$$

Again, Eqs. 41 and 49 are used for solving V_u and σ by the graphic method and the ultimate load P_u is then determined by Eq. 35.

Because the tension (bottom) flange is capable of strain hardening, and contributes a large portion of the ultimate moment of the cross section, the moment capacity computed without considering the hardening effects underestimates the strength. To incorporate the strain-hardening contribution of the bottom flange, the yield stress σ_{bf}^{y} in Eqs. 42g and 46f can be replaced by the strain-hardening stress σ_{bf}^{st}. All other equations for the evaluation of ultimate shear capacity V_u remain the same. However, since σ_{bf}^{st} is dependent on the strain, the solving of V_u/V_p must be by repetition.

3. GIRDERS UNDER SHEAR AND NEGATIVE BENDING

A composite box girder subjected to negative bending is shown in Fig. 11. Based on the results of elastic analysis and experiments (Ref. 17), the partial deck thickness in conjunction with the equivalent top flange width w_{e1} are adopted for stress evaluation up to web buckling. Thereafter, only the reinforcing bars in w_{e1} are considered effective. For the bottom, compressive flange with adequate longitudinal and transverse stiffeners to prevent local buckling[22], the equivalent width w_{e2} by shear lag analysis is assumed. If the longitudinal stiffeners are insufficiently provided, an effective width b_{e2} may be computed[23] and adopted. Because the effective width is stress dependent, that computed at yield stress is conservatively used in this analysis for the web buckling and post-buckling stages, flange failure, or full plastification of the cross section.

3.1 Strength by Web Failure

For each half of the effective box girder (Fig. 11), the web tension field shear capacity V_t and the locations of the interior plastic hinges in the flanges, c_1 and c_2, are computed by the same formulas (Eqs. 6, 8 and 9) as derived for the positive bending condition. However, the axial stresses and forces at the plastic hinges are different and have to be computed.

At the onset of web buckling, the normal stress at the corner hinge D of the bottom flange (Fig. 11) is computed by

$$\sigma_{bf}^{cl} = \frac{V_{cr}\,(L_1 - z_1 - a)y_{bf}}{I_x/2} \tag{50a}$$

and that at the interior hinge F is by

$$\sigma_{bf}^{il} = \frac{V_{cr}\,(L_1 - z_1 - a + c_2)y_{bf}}{I_x/2} \tag{50b}$$

where

V_{cr} = shear buckling strength of the panel ABCD of one web,

z_1 = distance from the left support to the left boundary of the panel in consideration,

y_{bf} = distance from the mid-thickness of the bottom flange to neutral axis of the effective box girder cross section, and

I_x = moment of inertia, computed using the partial deck thickness about the horizontal, centroidal (x) axis of the same effective box girder cross section.

Since the concrete deck is subjected to tension, the axial forces induced in the deck are assumed to be taken only by the reinforcing bars and the top steel flanges. The elastic centroid of the reinforcing bars and top steel flanges is shown in Fig. 12 and is located by

$$\bar{t}_{ec} + \frac{A_{s1}(t_c - t_1 + 0.5\ t_{tf}) + A_{s2}(t_2 + 0.5\ t_{tf})}{A_{ts}} \tag{51}$$

where

$\bar{t}_{ec}$ = distance from the mid-thickness of the top steel flange to the elastic centroid, and

$A_{ts} = A_{tf} + A_{s1} + A_{s2}$, the sum of the areas of one top steel flange and all the reinforcing bars in the width w_{el}.

At the corner hinge B the axial force in the width w_{el} is computed by

$$F_{cf}^{cl} = \frac{V_{cr}\ (L_1 - z_1)(y_{tf} + \bar{t}_{ec})}{I_x/2} \cdot A_{ts} \tag{52a}$$

and at the interior hinge E by

$$F_{cf}^{il} = \frac{V_{cr}\ (L_1 - z_1 - c_1)(y_{tf} + \bar{t}_{ec})}{I_x/2} \cdot A_{ts} \tag{52b}$$

Above the web buckling load, the axial forces due to tension field action at the corner hinges D and B (Fig. 11) are given by Eqs. 13 and 14. Those at the interior hinges F and E are computed from Eqs. 15.

Equilibrium of external moment creates normal forces F_{cf}^{c2}, F_{cf}^{i2}, F_{bf}^{c2} and F_{bf}^{i2} at the corner and interior hinges of the top (tension) and the bottom (compression) flanges. The forces F_{cf}^{c2} and F_{cf}^{i2} are assumed to be at the plastic centroid of the area consisting of one top steel flange and the reinforcing bars (A_{s1} and A_{s2}) in the width w_{el}. The plastic centroid is located by

$$\bar{t}_{pc} = \frac{\sigma_{s1}^{y} A_{s1}(t_c - t_1 + 0.5\, t_{tf}) + \sigma_{s2}^{y} A_{s2}(t_2 + 0.5\, t_{tf})}{F_{cf}^{u}} \tag{53a}$$

$$F_{cf}^{u} = \sigma_{s1}^{y} A_{s1} + \sigma_{s2}^{y} A_{s2} + \sigma_{tf}^{y} A_{tf} \tag{53b}$$

where

$\bar{t}_{pc}$ = distance from the mid-thickness of top steel flange to the plastic centroid, and

F_{cf}^{u} = the ultimate concentric load of the area A_{ts}.

The forces created by the moment equilibrium are then obtained from the moment at the respective hinge locations as follows:

$$F_{bf}^{c2} = \frac{V_t\,(L_1 - z_1 - a)}{b' + \bar{t}_{pc}} \tag{54a}$$

$$F_{bf}^{i2} = \frac{V_t\,(L_1 - z_1 - a + c_2)}{b' + \bar{t}_{pc}} \tag{54b}$$

$$F_{cf}^{c2} = \frac{V_t\,(L_1 - z_1)}{b' + \bar{t}_{pc}} \tag{54c}$$

$$F_{cf}^{i2} = \frac{V_t (L_1 - z_1 - c_1)}{b' + \bar{t}_{pc}} \tag{54d}$$

The total normal stress induced at the web buckling and post-buckling stages in the bottom flange at the corner hinge D is

$$\sigma_{bf}^{c} = \sigma_{bf}^{c1} + \frac{F_{bf}^{c2} + H_{bf}^{c}}{A_{bf}} \tag{55a}$$

and that at the interior hinge F is

$$\sigma_{bf}^{i} = \sigma_{bf}^{i1} + \frac{F_{bf}^{i2} + H_{bf}^{i}}{A_{bf}} \tag{55b}$$

where

$A_{bf} = t_{bf} \; b_{e2} + A_{st}$, the bottom flange area in the effective width b_{e2} plus the areas of the longitudinal stiffeners, if any, or

$A_{bf} = t_{bf} \; w_{e2} + A_{st}$, if applicable.

The modified plastic moments at the hinges of the bottom flange can be computed by sutstituting Eqs. 55 into Eq. 7.

What remains to be established for the evaluation of tension field shear capacity V_t is the equations for the ultimate moment capacities at the hinges of the top (tension) flange. At the corner hinge B, the contribution of concrete is ignored in computing the ultimate moment capacity because most of the deck is in tension. Figure 12 depicts the strain and force diagrams of the corner hinge. By the same procedure

as employed previously for composite box girders under shear and positive bending, the following equations are obtained:

$$k_u = 1 - \frac{\epsilon_{s1}^u}{\epsilon_{tf} + \epsilon_{s1}^u} \tag{56}$$

$$T_{s1} = \sigma_{s1}^y A_{s1} \tag{57a}$$

$$T_{s2} = \sigma_{s2} A_{s2} \tag{57b}$$

$$C_{tf} = \sigma_{tf} A_{tf} \tag{57c}$$

where the forces T_{s1}, T_{s2} and C_{tf} are those contributed by the steel reinforcing bars and the top steel flange in the width w_{el}, and

$$\sigma_{tf} = \sigma_{s1}^y \frac{A_{s1}}{A_{tf}} + \sigma_{s2} \frac{A_{s2}}{A_{tf}} - \frac{F_{cf}^{c1} + F_{cf}^{c2} - H_{tf}^c}{A_{tf}} \tag{58}$$

The neutral axis can be located by trial using Eq. 58. A value of σ_{s2} is assumed. The top steel flange stress σ_{tf} is then computed, from which the strain ϵ_{tf} is obtained. The location of the neutral axis can be calculated by Eq. 56, and the resulting strain ϵ_{s2} checked against the assumed σ_{s2} value. The procedure is repeated until satisfactory results are acquired. The ultimate moment capacity at hinge B in the width w_{el} is

$$\begin{aligned} M_u^c = {} & T_{s1} (1 - k_u) t_4 + T_{s2} (t_2 + 0.5\, t_{tf} - k_u\, t_4) \\ & + (C_{tf} - H_{tf}^c)\, k_u\, t_4 - F_{cf}^{c1} (\bar{t}_{ec} - k_u\, t_4) \\ & - F_{cf}^{c2} (\bar{t}_{pc} - k_u\, t_4) \end{aligned} \tag{59}$$

At the interior hinge E, the concrete is mostly subjected to compression and is assumed to be effective. The ultimate moment capacity of the hinge is computed in accordance with three different strain conditions as shown in Fig.13:

(a) $\epsilon_{tf} = \epsilon_{tf}^{u}$ and $\epsilon_c \leq \epsilon_{cy}$;

(b) $\epsilon_{tf} = \epsilon_{tf}^{u}$ and $\epsilon_{cy} < \epsilon_c < \epsilon_{cu}$; and

(c) $\epsilon_c = \epsilon_{cu}$.

Where ϵ_{tf}^{u} is the rupture strain of the top steel flange. For case (a) when the top steel flange reaches rupture strain and the top fiber strain of concrete is below its idealized yield value (Fig. 13a) the location of neutral axis and the hinge forces are given by the following equations:

$$k_u = 1 - \frac{\epsilon_{tf}^{u}}{\epsilon_{sl} + \epsilon_{tf}^{u}} \tag{60}$$

$$C_c = 0.5\, f_c\, (k_u\, t_4 + t_1)\, w_{el} \tag{61a}$$

$$C_{sl} \doteq (\sigma_{sl} - f_c)\, A_{sl} \tag{61b}$$

$$T_{s2} = \sigma_{s2}\, A_{s2} \tag{61c}$$

$$T_{tf} = \sigma_{tf}^{y}\, A_{tf} \tag{61d}$$

Also, from equilibrium of the forces,

$$\sigma_{s1} = \frac{0.5\, f_c\, \epsilon_{tf}^{u}}{\epsilon_{s1} + \epsilon_{tf}^{u}} \cdot \frac{t_4\, w_{e1}}{A_{s1}} + f_c - 0.5\, f_c \frac{t_3\, w_{e1}}{A_{s1}}$$

$$+ \sigma_{s2} \frac{A_{s2}}{A_{s1}} + \sigma_{tf}^{y} \frac{A_{tf}}{A_{s1}} - \frac{F_{cf}^{i1} + F_{cf}^{i2} - H_{tf}^{i}}{A_{s1}} \tag{62}$$

Again, the neutral axis can be located by trial. A procedure is as the following:

(1) Assume f_c and σ_{s2}.

(2) Determine σ_{s1} and ϵ_{s1} using Eq. 62 and the idealized σ - ϵ relationship of the bars A_{s1}.

(3) Locate the neutral axis by Eq. 60.

(4) Compute ϵ_c and ϵ_{s2} and obtain the corresponding stresses, f_c and σ_{s2}, from their individual idealized σ - ϵ relationship.

(5) Check the computed and assumed stresses f_c and σ_{s2}, and repeat the procedure until satisfactory results are obtained.

The ultimate moment at the interior hinge E in the width w_{e1} is given as

$$M_u^i = \frac{2}{3} C_c (k_u t_4 + t_1) + C_{s1} k_u t_4 + T_{s2} [(1 - k_u)t_4 - 0.5\, t_{tf} - t_2] + (T_{tf} + H_{tf}^{i})(1 - k_u)t_4 - F_{cf}^{i1} [(1 - k_u)t_4 - \bar{t}_{ec}] - F_{cf}^{i2} [(1 - k_u)t_4 - \bar{t}_{pc}] \tag{63}$$

For the case of $\epsilon_{tf} = \epsilon_{tf}^{u}$ and $\epsilon_{cy} < \epsilon_c < \epsilon_{cu}$ (Fig. 13b), Eq. 60 remains applicable. If it is defined

$$t_5 = \frac{\epsilon_{cy}}{\epsilon_{s1} + \epsilon_{tf}^{u}} \cdot t_4 \tag{64}$$

the horizontal forces at the hinge are

$$C_{c1} = f_c' (k_u t_4 - t_5 + t_1) w_{e1} \tag{65a}$$

$$C_{c2} = 0.5 f_c' t_5 w_{e1} \tag{65b}$$

$$C_{s1} = (\sigma_{s1} - f_c') A_{s1} \tag{65c}$$

$$T_{s2} = \sigma_{s2} A_{s2} \tag{65d}$$

$$T_{tf} = \sigma_{tf}^{y} A_{tf} \tag{65e}$$

From the equilibrium of horizontal forces, it is obtained

$$\sigma_{s1} = f_c' \frac{\epsilon_{tf}^{u} + 0.5 \epsilon_{cy}}{\epsilon_{s1} + \epsilon_{tf}^{u}} \cdot \frac{t_4 w_{e1}}{A_{s1}} + f_c' - f_c' \frac{t_3 w_{e1}}{A_{s1}}$$

$$+ \sigma_{s2} \frac{A_{s2}}{A_{s1}} + \sigma_{tf}^{y} \frac{A_{tf}}{A_{s1}} - \frac{F_{cf}^{i1} + F_{cf}^{i2} - H_{tf}^{i}}{A_{s1}} \tag{66}$$

The neutral axis can be located by assuming σ_{s2} in Eq.66 and following the same trial procedure as employed for Eq.62. The ultimate moment capacity at hinge E in the width w_{e1} is

$$M_u^i = 0.5 C_{c1} (k_u t_4 + t_1 + t_5) + \frac{2}{3} C_{c2} t_5 + C_{s1} k_u t_4$$
$$+ T_{s2}[(1 - k_u)t_4 - 0.5 t_{tf} - t_2] + (T_{tf} + H_{tf}^{i})(1 - k_u)t_4 - F_{cf}^{i1} [(1 - k_u)t_4 - \bar{t}_{ec}]$$
$$- F_{cf}^{i2} [(1 - k_u)t_4 - \bar{t}_{pc}] \tag{67}$$

For the case where the concrete is crushed, $\epsilon_c = \epsilon_{cu}$ (Fig. 13c), the equations are

$$k_u = \frac{0.003}{\epsilon_{tf} + 0.003} \tag{68}$$

$$C_c = 0.85\, f_c' \,\beta_1\, k_u\, t_3\, w_{el} \tag{69a}$$

$$C_{s1} = (\sigma_{s1} - 0.85\, f_c')\, A_{s1} \tag{69b}$$

$$T_{s2} = \sigma_{s2}\, A_{s2} \tag{69c}$$

$$T_{tf} = \sigma_{tf}\, A_{tf} \tag{69d}$$

and

$$\sigma_{tf} = \frac{0.00255\, f_c'\, \beta_1}{\epsilon_{tf} + 0.003} \cdot \frac{t_3\, w_{el}}{A_{tf}} + (\sigma_{s1} - 0.85\, f_c') \frac{A_{s1}}{A_{tf}} - \sigma_{s2} \frac{A_{s2}}{A_{tf}} + \frac{F_{cf}^{i1} + F_{cf}^{i2} - H_{tf}^{i}}{A_{tf}} \tag{70}$$

The neutral axis can be determined by the same trial procedure as that for Eq. 21. The ultimate moment capacity at the interior hinge E in w_{el} is given as

$$M_u^i = C_c(1 - 0.5\,\beta_1)\, k_u\, t_3 + C_{s1}(k_u\, t_3 - t_1) + T_{s2}(t_c - t_2 - k_u\, t_3) + (T_{tf} + H_{tf}^{i})(1 - k_u)t_3 - F_{cf}^{i1}[(1 - k_u)t_3 - \bar{t}_{ec}] - F_{cf}^{i2}\,[(1 - k_u)t_3 - \bar{t}_{pc}] \tag{71}$$

When the expressions for the ultimate moment capacities at the hinges are derived, the interior hinge locations c_1 and c_2 can be determined by the same iterative process as that employed for a panel in the positive moment region.

Finally, the ultimate shear strength of the panel of one web (V_u) and the corresponding ultimate load (P_u) causing failure of a box panel of two webs (Fig. 11) are respectively

$$V_u = V_{cr} + V_t \tag{72}$$

$$P_u = 2\,\overline{V}_u \tag{73}$$

3.2 Strength by Flange Failure

At end $\overline{BC}$ of panel ABCD in Fig. 11, the bending moment is higher than that at end $\overline{AD}$. The steel bottom flange or the effective top tension flange of reinforcing bars plus the top steel flanges may yield at the end of higher moment prior to the failure of the web.

At web panel buckling the normal stress and force in the bottom flange and in the effective top tension flange are, respectively,

$$\sigma_{bf}^{cr} = \frac{V_{cr}\,(L_1 - z_1)y_{bf}}{I_x/2} \tag{74a}$$

$$F_{cf}^{cr} = \frac{V_{cr}\,(L_1 - z_1)(y_{tf} + \overline{t}_{pc})}{I_x/2} \cdot A_{ts} \tag{74b}$$

The additional compressive force to cause yielding of the bottom flange in the effective width b_{e2} (or w_{e2}) is

$$\Delta F_{bf} = (\sigma_{bf}^{y} - \sigma_{bf}^{cr})\,A_{bf} \tag{75a}$$

and the additional tensile force to cause yielding of the effective tension flange in w_{el} is

$$\Delta F_{cf} = F_{cf}^{u} - F_{cf}^{cr} \tag{75b}$$

where F_{cf}^{u} is from Eq. 53b. The smaller value of ΔF_{bf} and ΔF_{cf}, designated as ΔF, controls the flange failure. Thus, the shear capacity contributed by the failure of the flange is

$$V_f = \frac{\Delta F(b' + \bar{t}_{pc})}{L_1 - z_1} \tag{76}$$

The ultimate shear capacity of the panel of one web is

$$V_u = V_{cr} + V_f \tag{77}$$

and the ultimate load, P_u, is given by Eq. 73.

3.3 Strength by Full Plastification of the Cross Section

If the top steel flanges yield in tension before the webs buckle, full plastification of the cross section may result. The web shear strength and the yield condition as given by Eqs. 40 and 41 are still applicable.

Figure 14 depicts the case of plastification where the neutral axis is in the webs. The forces at full plastification are:

$$T_{s1} = \sigma_{s1}^{y} A_{s1} \tag{78a}$$

$$T_{s2} = \sigma_{s2}^{y} A_{s2} \tag{78b}$$

$$T_{tf} = \sigma_{tf}^{y} A_{tf} \tag{78c}$$

$$T_w = \sigma t_w (k_u d - t_c - t_{tf}) \tag{78d}$$

$$C_w = \sigma t_w [(1 - k_u)d - 0.5\, t_{bf}] \tag{78e}$$

$$C_{bf} = \sigma_{bf}^{y} A_{bf} \tag{78f}$$

These forces are acting in half of the effective cross section. The neutral axis is located by

$$k_u = k_1 - \frac{s_2}{\sigma} \tag{79a}$$

where k_1 is given by Eq. 43b, and

$$s_2 = \frac{1}{2d\, t_w} (T_{s1} - T_{s2} + T_{tf} - C_{bf}) \tag{79b}$$

The ultimate moment of half of the effective cross section is

$$M_u = (v_1 + v_2)\, \sigma - \frac{s_2}{\sigma} m_{13} + m_{14} \tag{80a}$$

where v_1 and v_2 have been given in Eqs. 44b and 44c, and

$$m_{13} = s_2\, t_w\, d^2 \tag{80b}$$

$$m_{14} = m_9 - m_{10} - m_{11} + m_{12} \tag{80c}$$

$$m_9 = T_{s1} (k_1 d - t_1) + T_{s2} (k_1 d - t_c - t_2) + T_{tf}(k_1 d - t_c - 0.5 t_{tf}) + C_{bf}(1 - k_1)d \tag{80d}$$

$$m_{10} = \frac{1}{2} s_2\, t_w\, d[(1 - 2k_1)d + t_c + t_{tf} - 0.5\, t_{bf}] \tag{80e}$$

$$m_{11} = \frac{1}{2} s_2\, t_w\, d(k_1 d - t_c - t_{tf}) \tag{80f}$$

$$m_{12} = \frac{1}{2} s_2\, t_w\, d[(1 - k_1)d - 0.5\, t_{bf}] \tag{80g}$$

The equilibrium of internal and external moments at the panel boundary $z = z_1$ (Fig. 11) gives

$$\frac{V_u}{V_p} = \frac{1}{V_p(L_1 - z_1)} \left[(v_1 + v_2)\ \sigma_{yw}\ \left(\frac{\sigma}{\sigma_{yw}}\right) - \frac{s_2\ m_{13}}{\sigma_{yw}} \left(\frac{\sigma_{yw}}{\sigma}\right) + m_{14}\right] \tag{81}$$

Equation 81 is limited by the yield condition of Eq. 41, and can be solved graphically for V_u and σ as described before. The ultimate load is twice the value of V_u (Eq. 73).

For composite box girders with normal cross-sectional configuration and geometry, it is unliely that the neutral axis of full plasticification is in the bottom flange. If this is the case, it can be analyzed by the same procedure as employed for the case where the neutral axis is in the webs.

4. LOCAL FAILURE OF FLANGES

4.1 Overall Buckling of Compression Flange

Thus far, all the equations for web failure, flange failure, and full plastification of a box girder cross section under negative bending moment have been derived on the assumption that the bottom flange is capable of attaining the yield stress at the longitudinal stiffeners. This requires that the longitudinal stiffeners be properly provided, that a compression flange panel between transverse stiffeners not buckle as a stiffened plate panel, and that the entire compression flange not buckle as a unit. These topics have been studied extensively [24,25] and are not unique to composite box girders. It suffices to assume here that no compression flange failure occurs prior to yielding.

4.2 Pull-out of Stud Shear Connectors

It has been assumed that complete composite action between the steel portion and the concrete deck can be developed through sufficient stud shear connectors. It has also been assumed that the composite deck can anchor the vertical components of the tension field forces. These vertical components induce tensile forces in the shear connectors. This, in turn, may cause pull-out of the stud connectors from the reinforced concrete deck by a shear cone mechanism.

If the concrete surrounding a stud shear connector has adequate space to develop a full shear cone as shown in Fig. 15a, the ultimate tensile capacity of the shear cone is[19]

$$P_{uc} = 4\, A_{fc}\sqrt{f_c'} \tag{82}$$

where

$A_{fc} = \sqrt{2}\pi\ L_e\ (L_e + D_s)$, the area of a full conical surface,

L_e = embedment length of the shear connectors,

D_s = diameter of the connector head, and

f_c' = concrete strength.

The reduction factor of 0.85 for concrete subjected to shear[21] is not included in Eq. 82. When the shear connectors are closely placed such that the shear cones overlap (Fig. 15b), the corresponding reduced ultimate tensile capacity of a partial shear cone is

$$RP_{uc} = 4\, A_{pc}\sqrt{f_c'} \tag{83}$$

where A_{pc} = area of the partial cone.

If n_r is the number of rows of shear connectors within the segment c_1 between the two plastic hinges E and B (Fig. 15c), n_s the number of shear connectors in each row, g_i the distance from ith row to the corner hinge B, P_s the force in one shear connector in the row farthest from B (the first row), and if it is assumed that the top steel flange rotates as a rigid bar about hinge B where a web transverse stiffener exists, then by the equilibrium of moment at B:

$$P_s = \frac{\sigma_t t_w c_1^2 \sin^2\phi}{2n_s \sum_{i=1}^{n_r} \frac{g_i^2}{g_1}} \tag{84}$$

If the computed c_1 indicates that the tension field extends over the entire panel at the web-to-deck junction ($c_1 \geq a$), then the maximum deflection between the steel top flange and the concrete deck is at mid-panel (Fig. 15d), and Eq. 84 becomes

$$P_s = \frac{\sigma_t t_w a^2 \sin^2\phi}{8n_s \sum_{i=1}^{n_r} \frac{g_i^2}{g_1}} \tag{85}$$

The force P_s must be smaller than P_{uc} or RP_{uc}, whichever is applicable, in order to avoid separation between the concrete deck and the top steel flanges through the formation of shear cones.

It is worth noting that the equivalent flange widths, w_{e1} and w_{e2}, used in this chapter are obtained from the procedure developed in Ref. 17 where no web buckling is involved. For the strength of a girder governed by web failure, web tension field develops in the panel in question. The portion of concrete deck and bottom flange within the length of that panel is subjected to the vertical components of the tension field stresses in addition to the normal forces developed for equilibrium with the external moment. Because of the pulling due to web tension field action, the equivalent widths at the plastic hinges in the flanges may be smaller than those obtained from the procedure

of Ref. 17. However, owing to lack of better information, the effect of the vertical pulling from the tension field on the equivalent widths of the flanges is neglected in the present derivations.

5. RESULTS AND COMPARISONS

The method developed in this report is for evaluating the ultimate strength of composite box girders subjected to flexural loading. It can be applied to composite plate girders, steel box girders, and unsymmetrical and hybrid steel plate girders as well. The experimental strength of two box girders are compared here with the results of computation according to the procedure developed in this report.

One composite box girder (D1) (Fig. 14)[4] was tested to failure by a symmetrical flexural load at midspan. The material properties of this girder are listed in Table 1. The analysis indicated that the bottom flange at midspan would yield before the buckling of web panel 7 or 8 and full plastification of the cross section would govern the strength. The neutral axis was in the concrete deck, thus Eqs. 46 to 49 were employed. An ultimate load of 254.1 kN (57.1 kips) for P_u was obtained. However, at this load the bottom flange was in the strain hardening range. By assuming that the onset of strain hardening was at 12 ε_{bf}^{y} (0.0126) and the hardening modulus was 4826.5 MN/m^2 (700 ksi), an ultimate load of 324.0 kN (72.8 kips) was obtained. This computed load is 6.3% lower than the measured value of 345.8 kN (77.7 kips). A further improvement to the computed value could be made by considering the strain-hardening effects in the webs.

A small steel box girder specimen (M2) was tested to failure in flexure[1,2]. The details of the specimen are shown in Fig. 17 and the material properties are listed in Table 1. The interior hinge locations c_1 and c_2 and the optimal tension field inclination angle ϕ_o are calculated to be:

Panel 4	Panel 5
c_1 = 62.7 mm (2.47 in.)	c_1 = 70.6 mm (2.78 in.)
c_2 = 18.3 mm (0.72 in.)	c_2 = 18.8 mm (0.74 in.)
$\phi_o = 36.7^o$	$\phi_o = 30.0^o$

The computed ultimate capacity of 10.59 kN (2.379 kips) is comparable to the measured value. The measured ultimate load lies between 10.46 kN (2.35 kips) and 11.79 kN (2.65 kips) because of relaxation of the solder joints of the specimen and nonzero strain rate. For this model box girder, an ultimate load of 10.50 kN (2.360 kips) was estimated in Ref. 1 using an approximate buckling strength computation. The buckling loads are computed here by using charts of buckling coefficient corresponding to the state of stresses at the web panel boundary[27]. The results of strength evaluation are listed in Table 2.

No other experimental study could be found in the literature on the ultimate strength of composite plate girders. It appears that testing of thin web composite plate girders and additional testing of composite box girders in flexure are needed for better confirmation of the theoretical development of this study.

6. SUMMARY AND CONCLUSIONS

This report presents a procedure of ultimate strength evaluation of rectangular composite box girders under flexural (bending and shear) without torsion. A single-cell rectangular box girder is considered as the sum of two parallel composite plate girders. Shear lag effects may be incorporated in determining the dimensions of composite plate girders.

In the ultimate strength evaluation, the buckling and post-buckling behavior of web panels are studied. Failure of the composite top flange and of the steel bottom flange under both positive or negative bending moment are considered. Full plastification of cross section is a possible mode of failure and is also studied.

For box and plate girders with slender webs, the post-buckling strength relies on the development of tension field action which depends on the bending rigidity of the composite deck and the steel bottom flange. Tension field strength is reached when the two flanges have developed plastic hinges and are pulled in by the tension field action. The ultimate strength of a slender-web plate girder is the sum of the web buckling strength and the post-buckling strength of tension field action.

Although comparison of computed and test results from two box girders indicates the applicability of the procedure of this study,

more tests need to be conducted for further confirmation of the theoretical development. Meanwhile, strength of common dimension composite box and plate girders may be estimated using this analytical procedure.

ACKNOWLEDGMENTS

The study of this report followed the working load range studies of a research project, "Strength of Rectangular Composite Box Girders", sponsored by the Pennsylvania Department of Transportation in conjunction with the Federal Highway Administration. This study is a part of work towards the Ph.D. degree of the first author under the guidance of the second author. The study and research project were conducted at the Civil Engineering Department and the Fritz Engineering Laboratory of Lehigh University, Bethlehem, Pennsylvania. The Chairman of the Department is Dr. David A. VanHorn and the Director of the Laboratory is Dr. Lynn S. Beedle.

Thanks are due the sponsors of the research project for their support, without it this study would not have been possible. To Professor A. Ostapenko, a member of the Ph.D. program committee and a coworker of the research project, sincere appreciation is extended. Thanks are also due all other members of the committee and of the research project. The help from Mrs. Dorothy Fielding in typing and processing this report is deeply appreciated.

TABLE 1. MATERIAL PROPERTIES OF SPECIMENS

(All stresses in MN/m^2 (ksi)

Properties \ Specimens			D1	M2
Steel	Yield Stress*	Small Top Flanges	213.9	224.4 (32.5)
		Webs		210.3 (30.5)
		Bottom Flange	(31.0)	216.1 (31.3)
	Young's Modulus of Elasticity		203,550 (29,500)	
	Shear Modulus of Elasticity		78,315 (11,350)	
	Poisson's Ratio		0.3	
Concrete Deck	Compressive Strength*		34.5 (5.0)	--
	Young's Modulus of Elasticity		25,530 (3700)	--
	Shear Modulus of Elasticity		10,902 (1580)	--
	Poisson's Ratio		0.17	--
Yield Stress of Deck Reinforcement*			483 (70)	--

TABLE 2 COMPARISON OF ULTIMATE STRENGTH

Box Girder - Panel	Computed Strength kN (kips)	Test Results kN (kips)
D1 - 7 or 8	324.0 (72.8)	345.8 (77.7)
M1 - 4	10.6 (2.38)	10.5 ~ 11.8 (2.35 ~ 2.65)
M2 - 5	10.9 (2.46)	

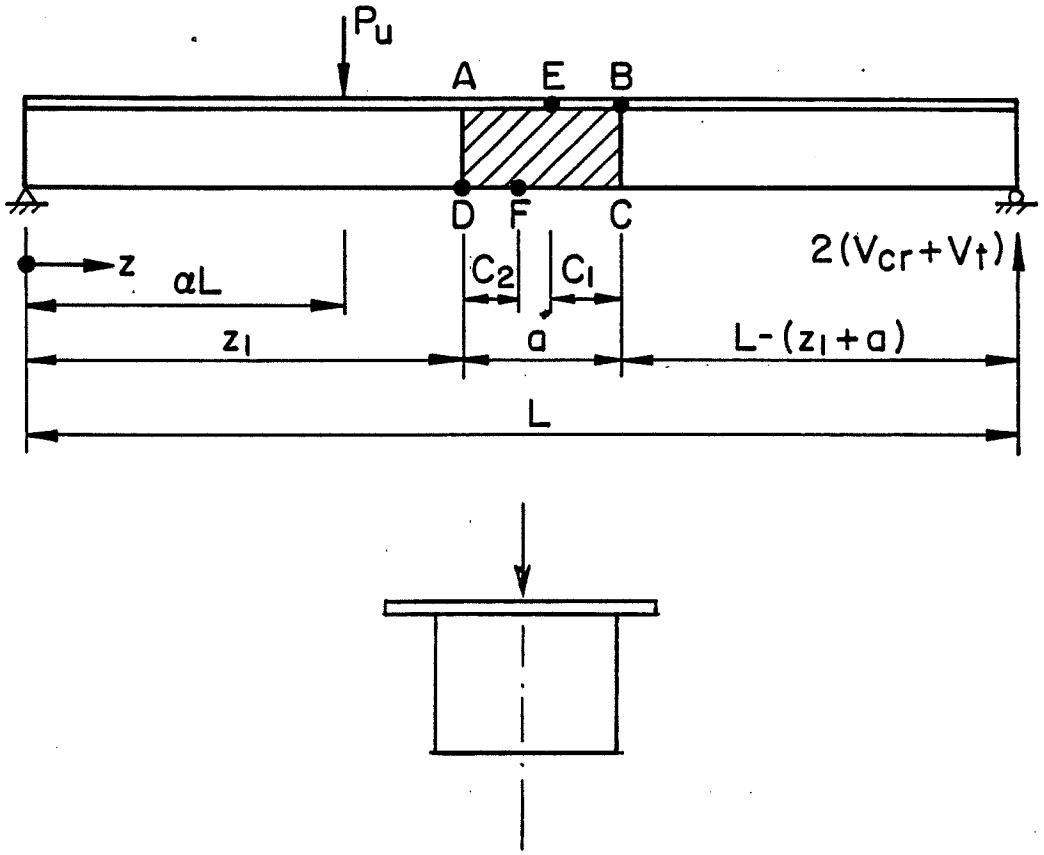

Fig. 1 A Box Girder in Positive Bending

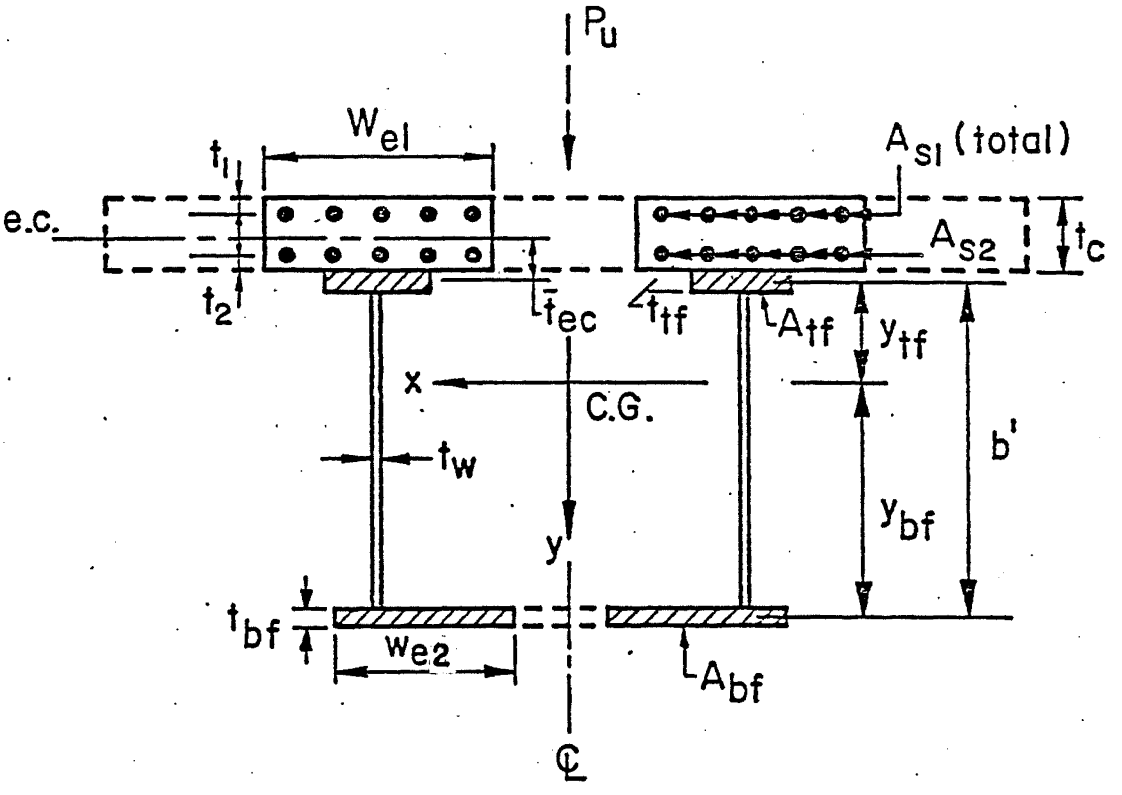

Fig. 2 Equivalent Cross Section

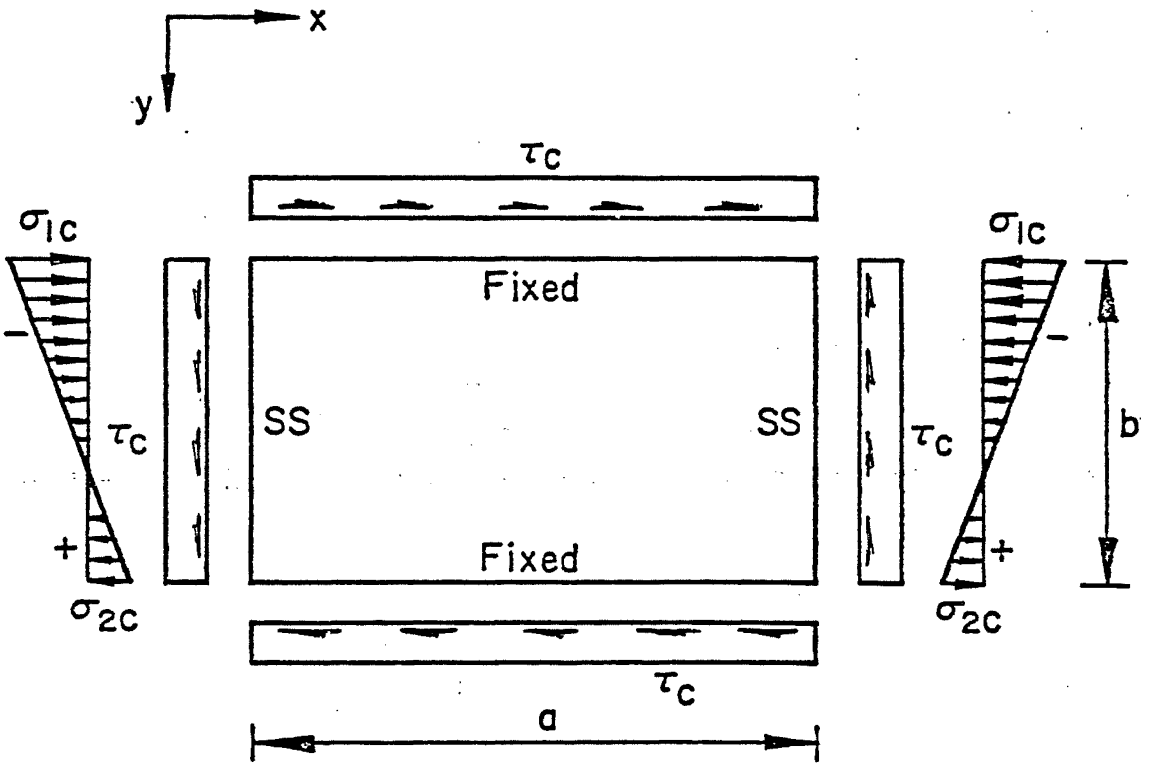

Fig. 3 A Plate under Combined Shearing and Normal Stresses at Critical State

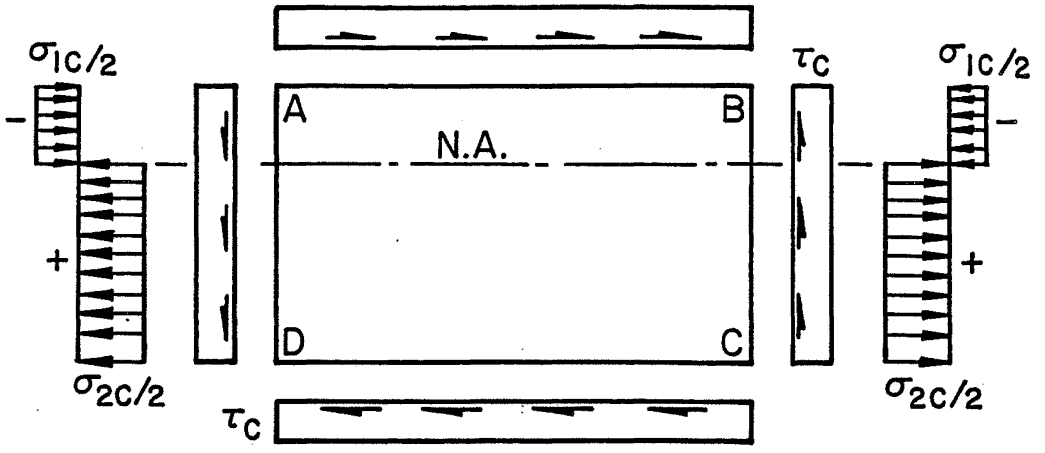

Fig. 4 Idealized State of Stress at Buckling

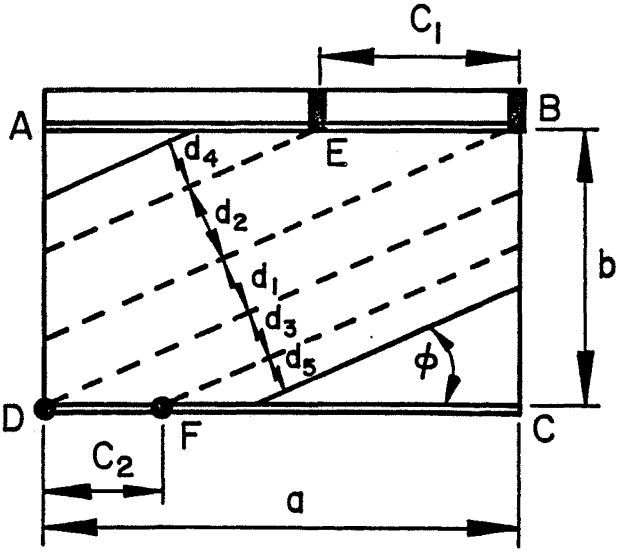

Fig. 5 Tension Field Model for Combined Shear and Bending

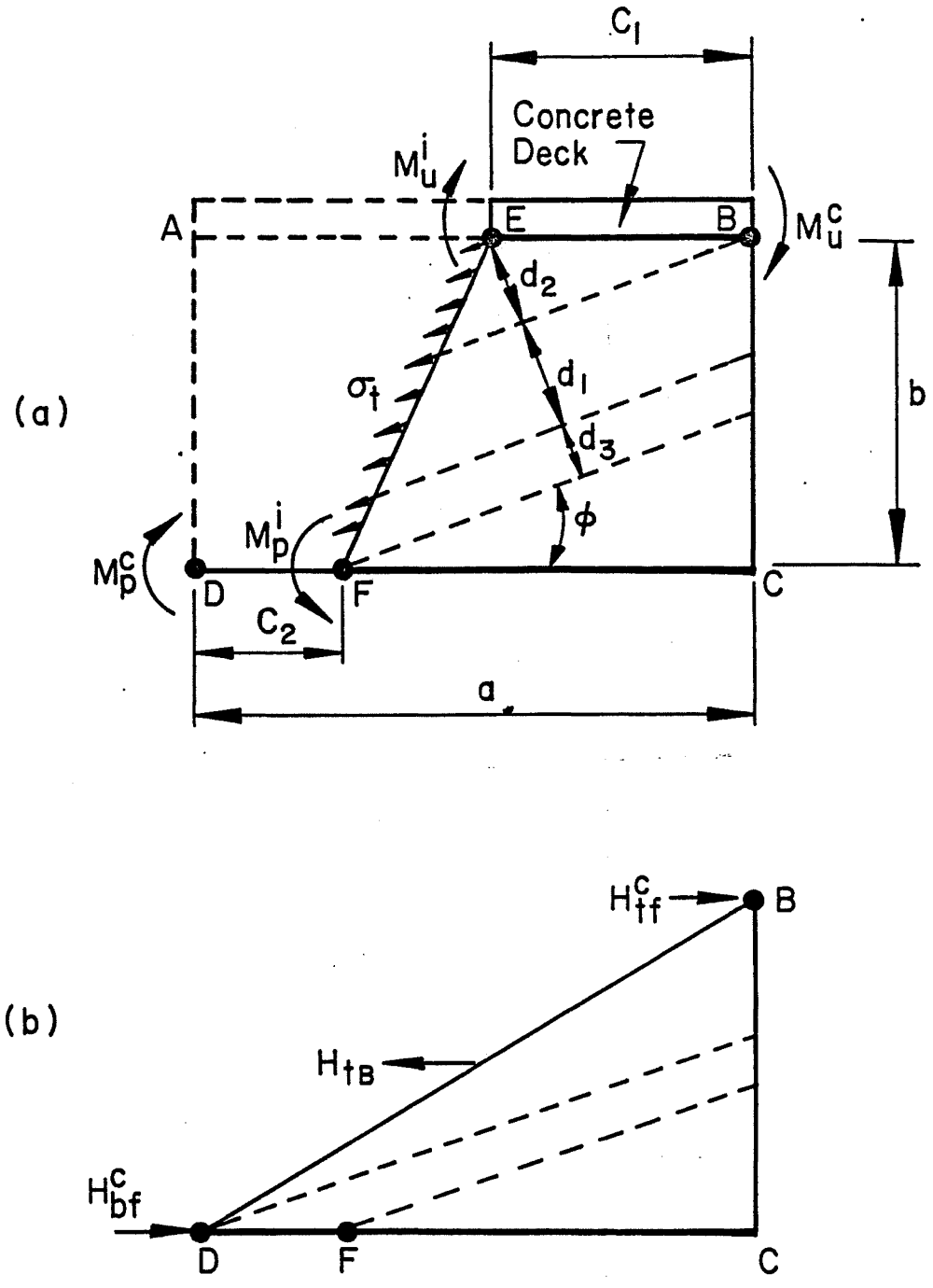

Fig. 6 Tensile Membrane Stresses and Horizontal Component of Basler Band

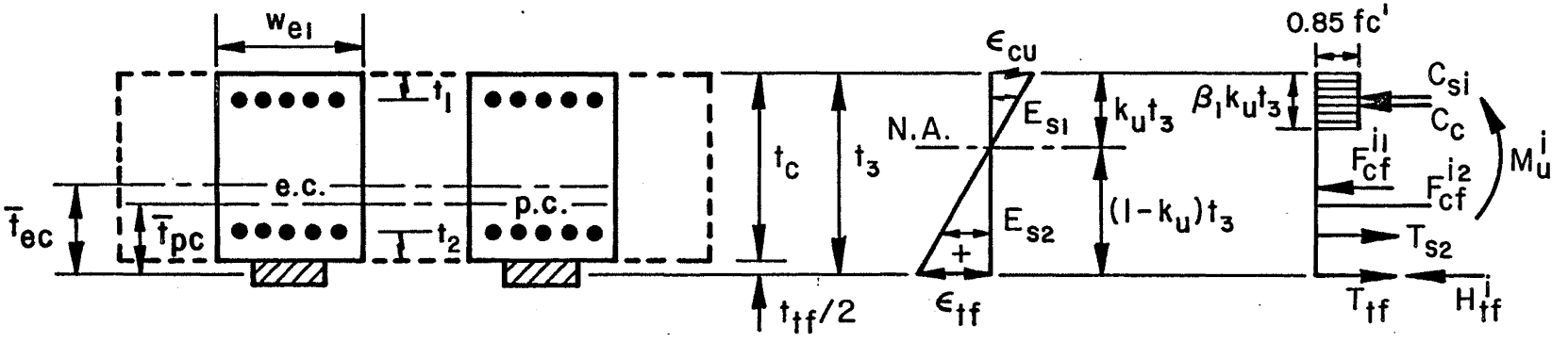

Fig. 7 Intermediate Plastic Hinge E (Panel in Positive Moment Region)

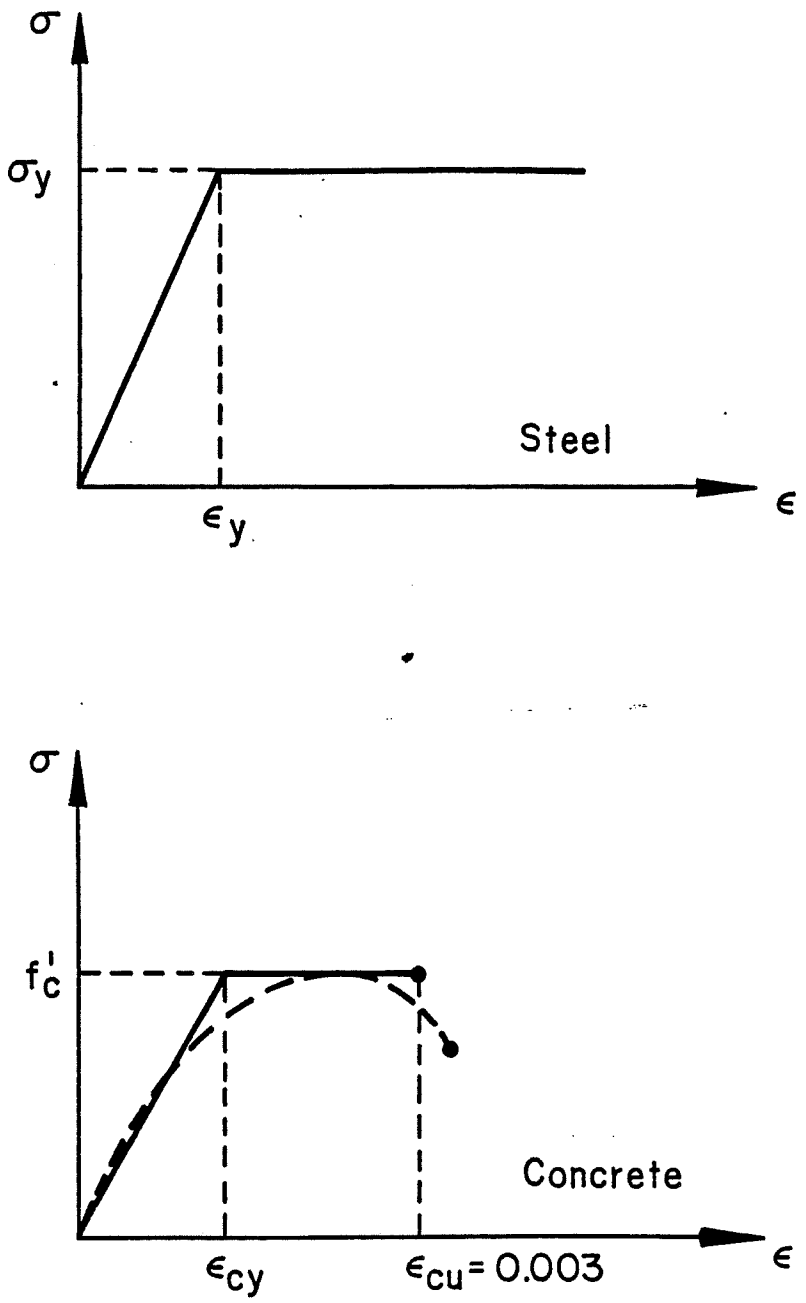

Fig. 8 Idealized Stress-Strain Relationship for Steel and Concrete

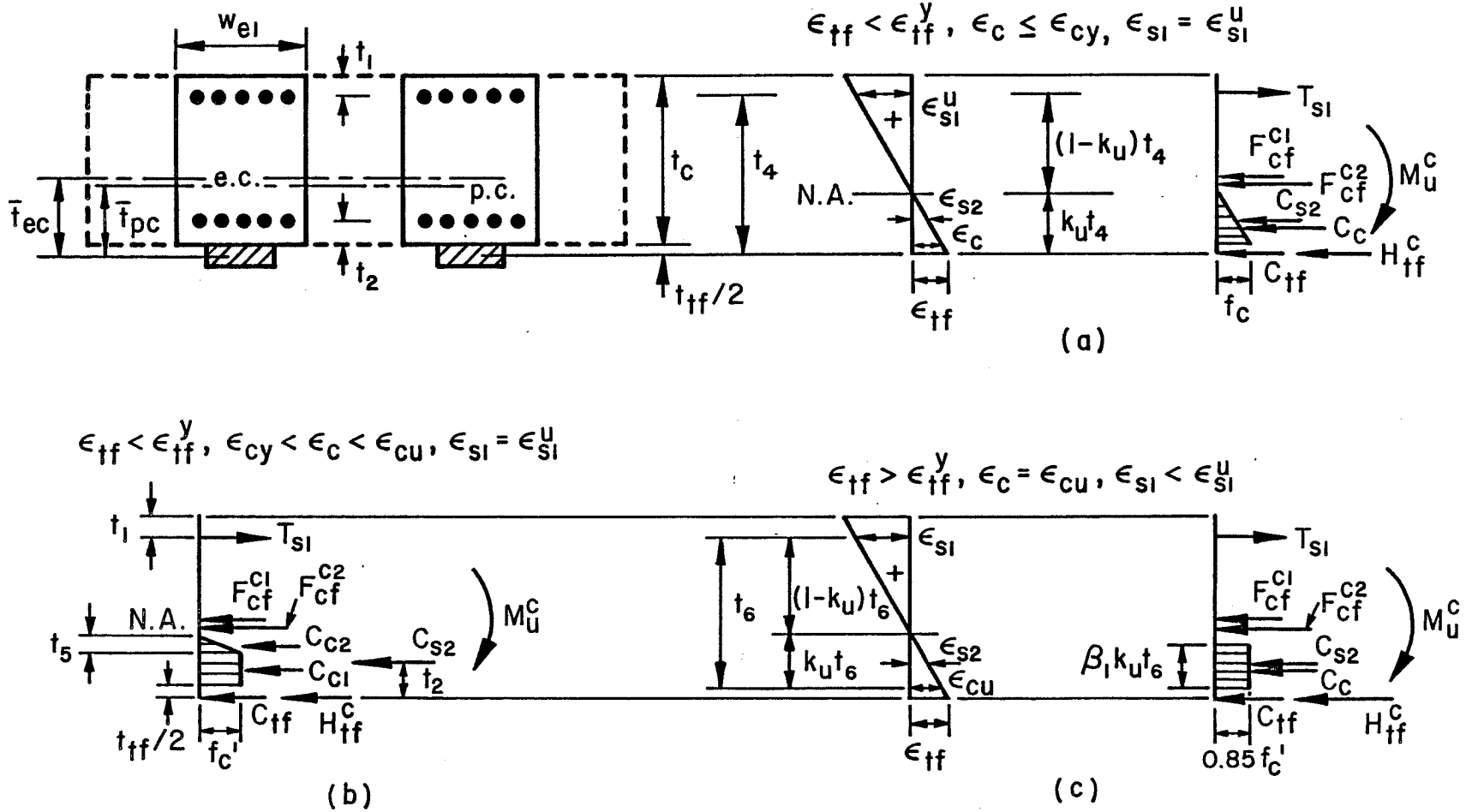

Fig. 9 Corner Plastic Hinge B (Panel in Positive Moment Region)

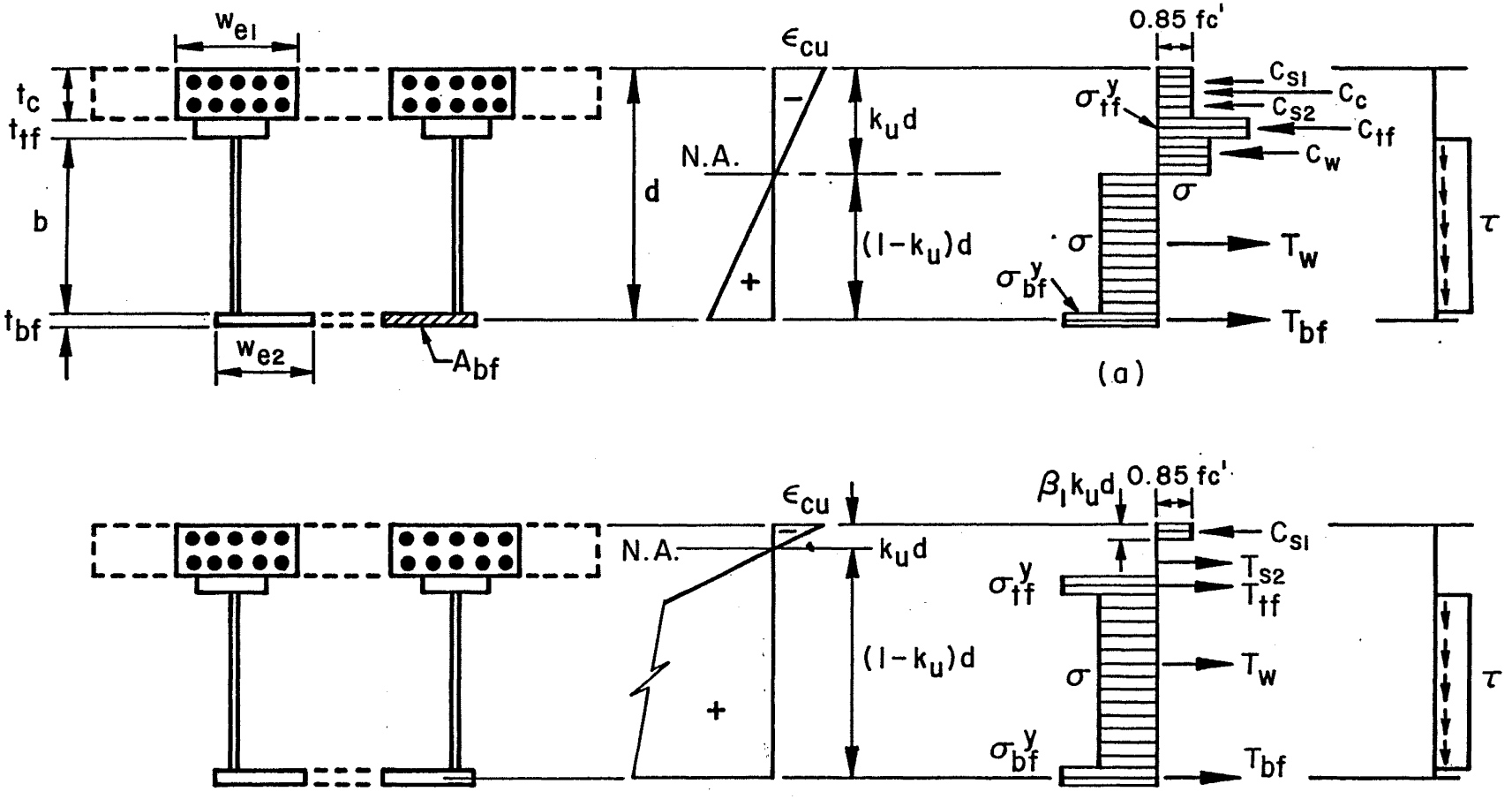

Fig. 10 Stress Distribution of Fully Plastified Cross Section Under Positive Bending

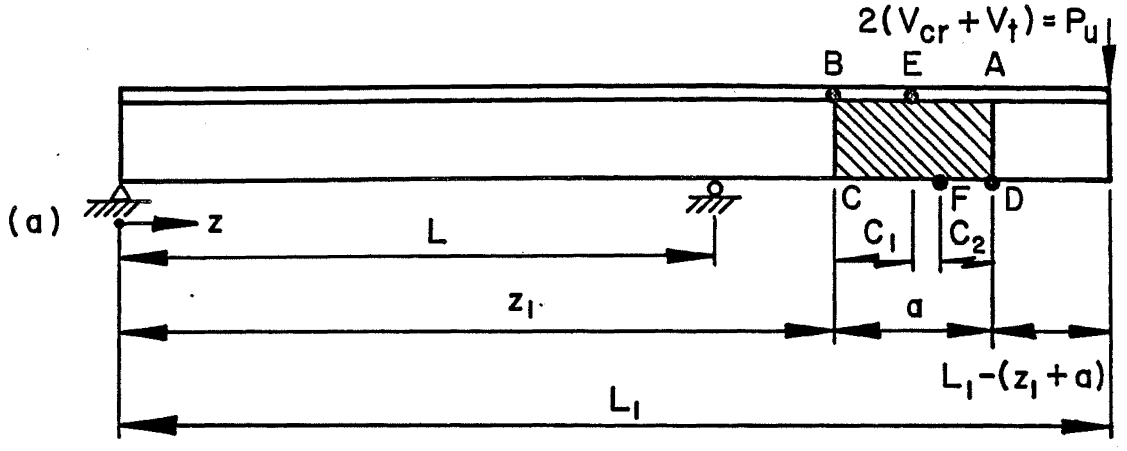

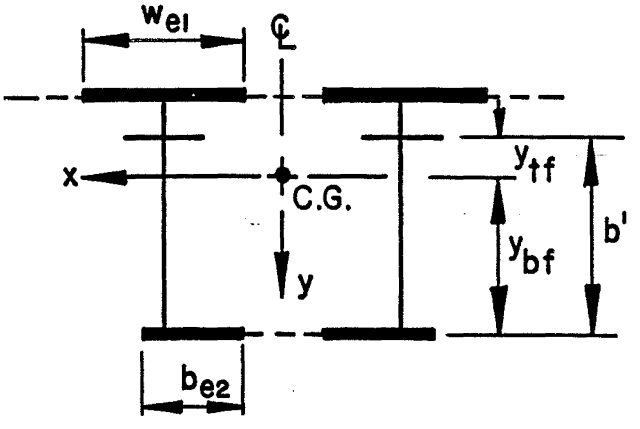

(b) Effective Cross-Section

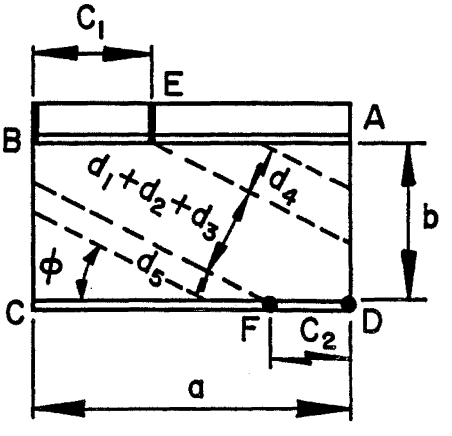

(c) Tension Field Model

Fig. 11 Web Panel in Negative Moment Region

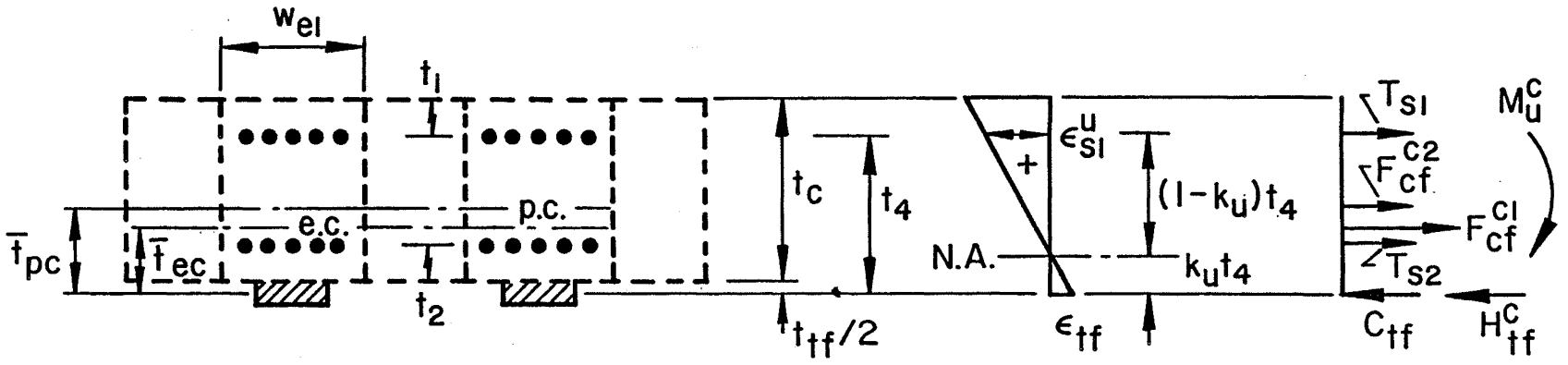

Fig. 12 Corner Plastic Hinge B (Panel in Negative Moment Region)

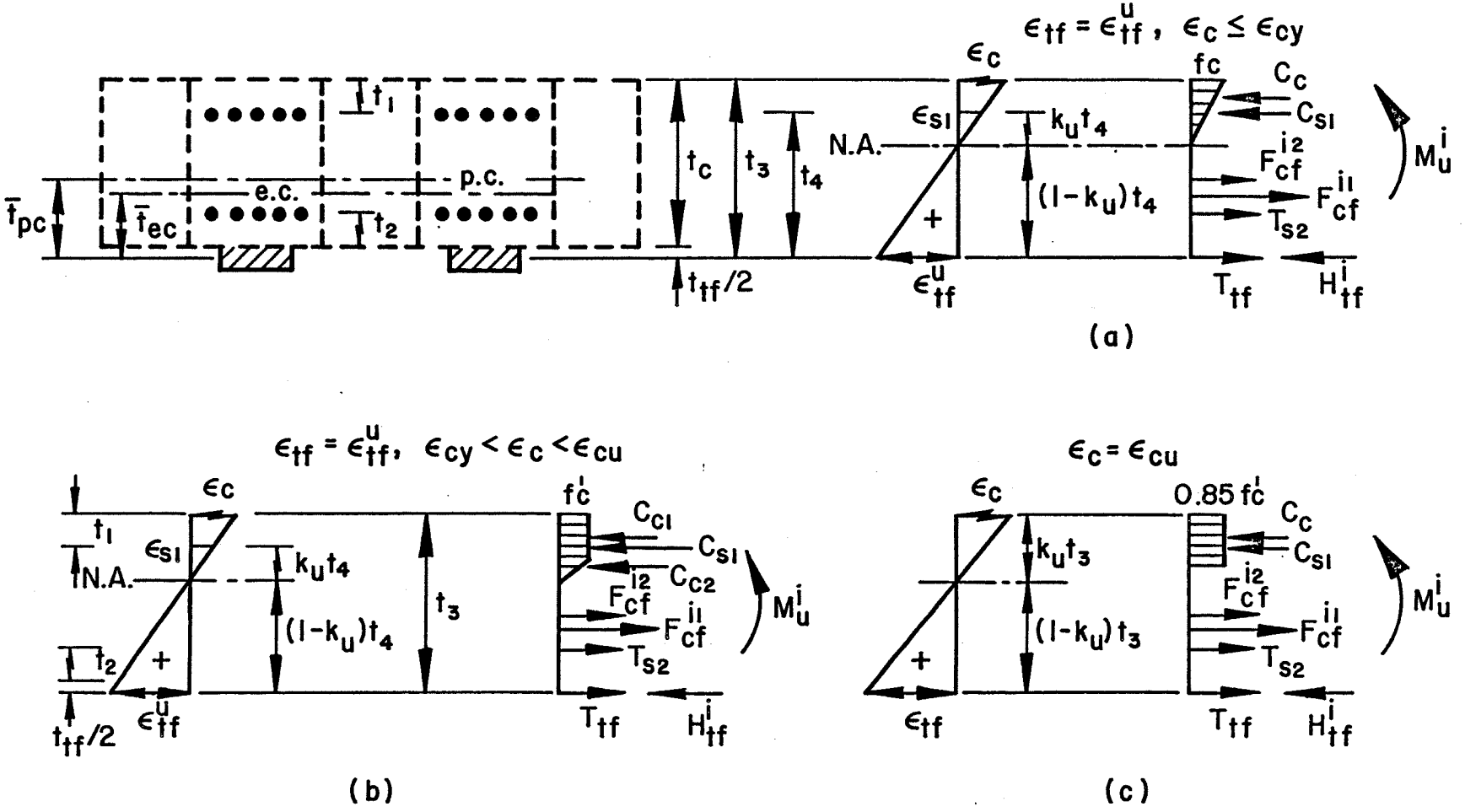

Fig. 13 Intermediate Plastic Hinge E (Panel in Negative Moment Region)

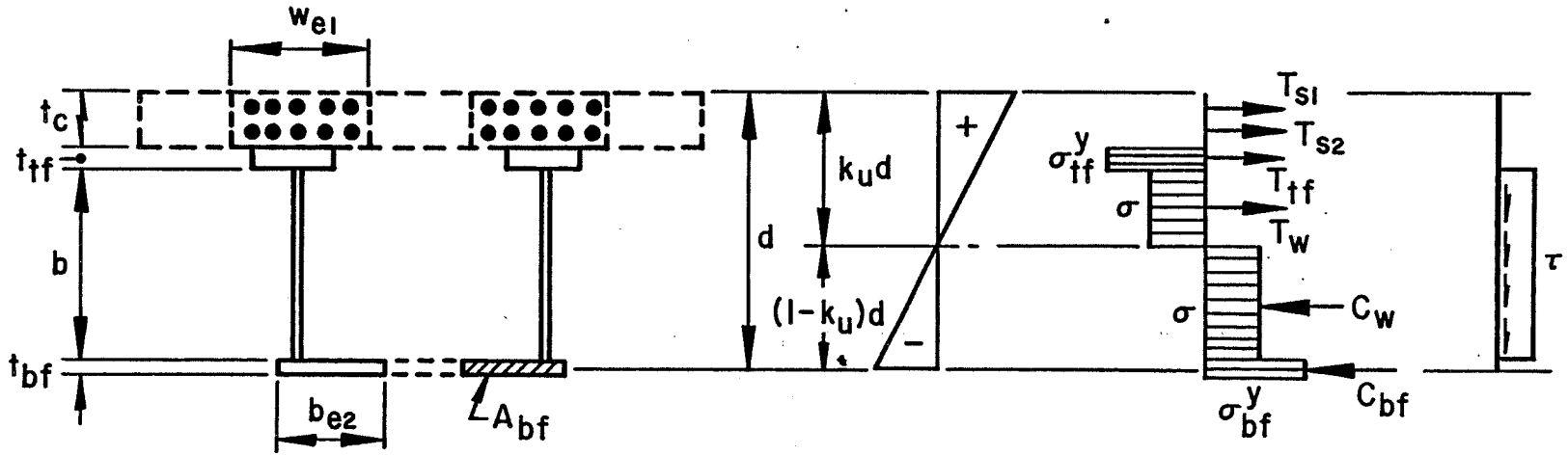

Fig. 14 Stress Distribution of Fully Plastified Cross Section Under Negative Bending

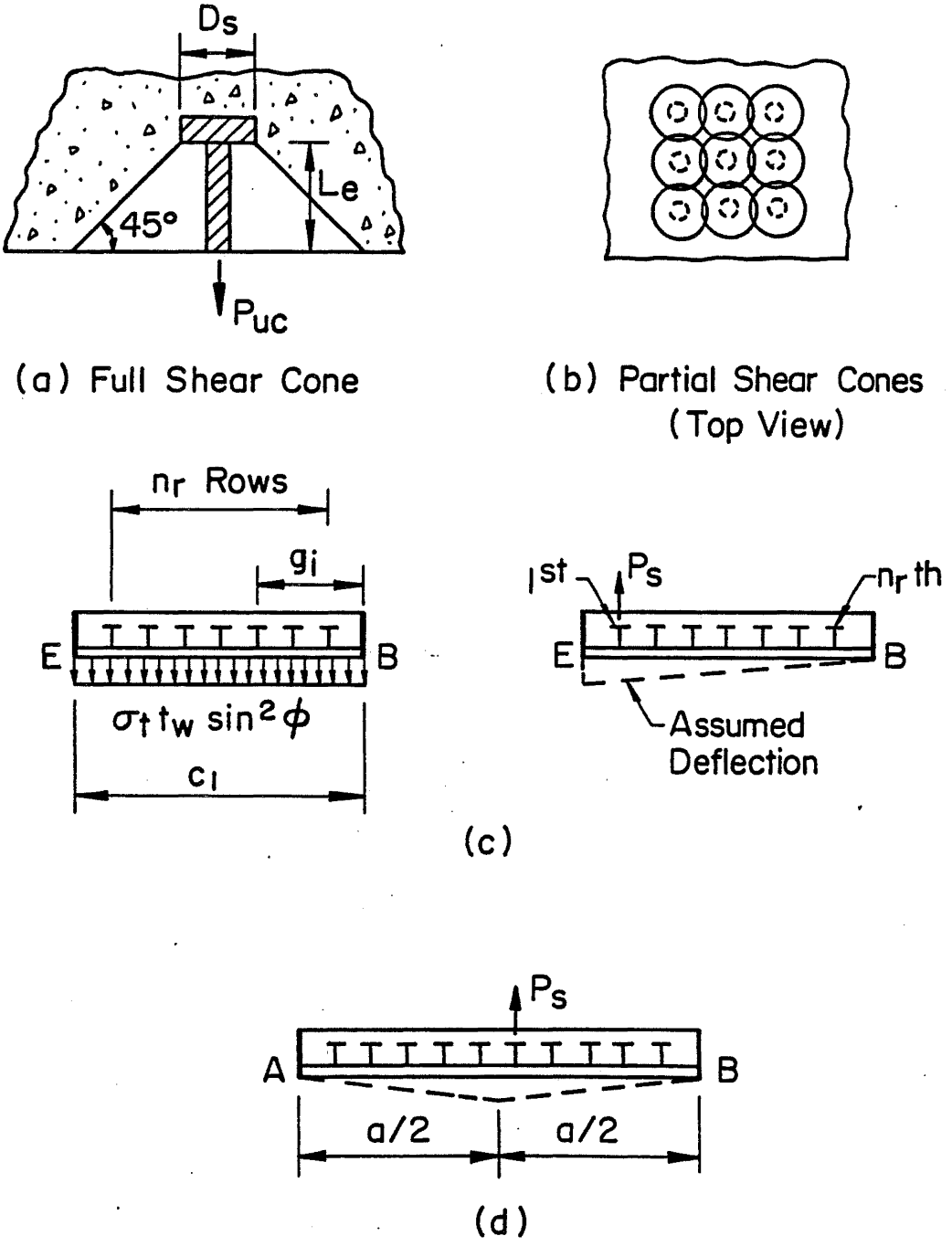

Fig. 15 Pull-out of Shear Connectors

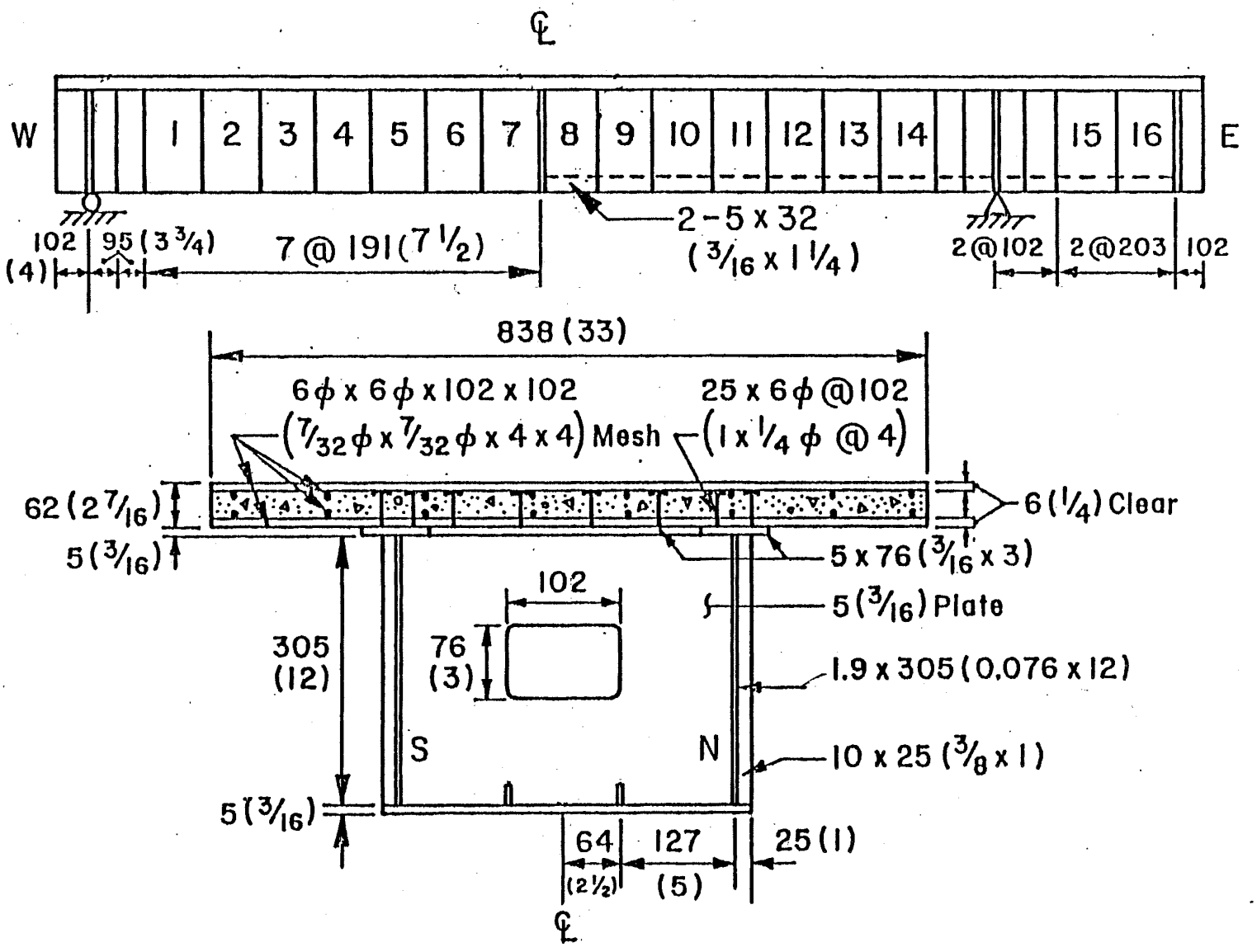

Fig. 16 Specimens D1 (all units in mm (in.)

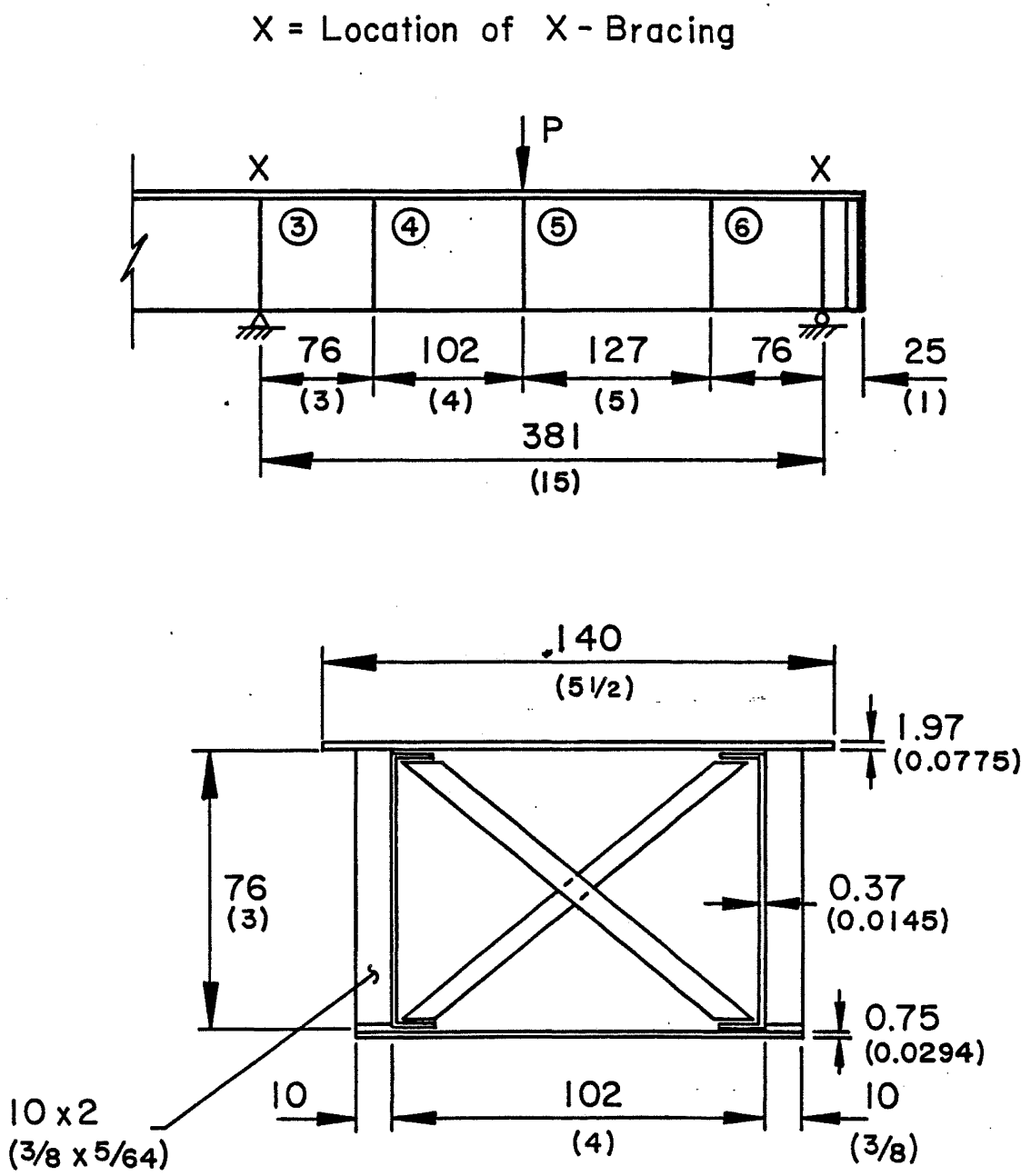

Fig. 17 Specimen M2 (All units in mm (in.))

NOTATIONS

A	Area
A_{bf}	Area of bottom steel flange in width w_{e2}
A_{fc}	Area of full conical surface of shear connector
A_g	Gross concrete area in width w_{el}
A_{pc}	Area of partial cone
A_{s1}, A_{s2}	Total area of longitudinal reinforcement of top and bottom layer, respectively, in w_{el}
A_t	Transformed area of width w_{el}
A_{tf}	Area of one top steel flange
A_{ts}	Total area of steel in top flange in w_{el}
A_w	Area of one web of box section
a	Panel length
b	Panel height, clear depth of web
b'	Distance between mid-thickness of top and bottom steel flanges
C_{bf}	Force in bottom flange
C_c	Total concrete force
C_{s1}, C_{s2}	Compressive force in reinforcing bars A_{s1}, A_{s2}
C_{tf}	Total compressive force in A_{tf}
C_w	Compressive force in web
c_1, c_2	Distance from corner plastic hinge to interior plastic hinge of top and bottom flange, respectively
D_s	Diameter of shear connector head

NOTATIONS (continued)

d_s'	Width of tension field
E_c, E_s	Elastic modulus of concrete and steel, respectively
F_{cf}^c, F_{cf}^i	Axial force at corner and interior hinge, respectively, in width w_{el} of concrete
F_{cf}^{cr}	Normal force in composite top flange at web buckling
F_{cf}^u	Ultimate concentrated load of top flange in width, w_{el}
f_c	Concrete stress at extreme fiber
f_c'	Compressive strength of concrete
g	Distance from corner hinge to a row of shear connectors
H_{bf}, H_{bf}^i	Horizontal normal force at corner hinge and interior hinge, respectively, in bottom flange, due to tension field
H_{tB}	Horizontal component of tension field force in width, d_1
H_{tf}^c, H_{tf}^i	Horizontal normal force at corner hinge and interior hinge, respectively, in top steel flange, due to tension field
I_x	Moment of inertia about horizontal centroidal axis of equivalent box section
k_s'	Notations (non-dimensional) for simplifying computation
k_u	Coefficient for determining neutral axis
L	Span length
L_e	Embedment length of shear connector
M_p	Plastic moment capacity of bottom flange of width, w_{e2}
M_p^c, M_p^i	Modified plastic moment at corner and interior hinge, respectively, of compression flange in width, w_{el}
M_u	Ultimate moment for half of box section

NOTATIONS (continued)

M_u^c, M_u^i	Ultimate moment at corner and interior hinge, respectively of compression flange in width, w_{e1}
m_s'	Notations of moment for simplifying computation
n	Modulus ratio, $n = E_s/E_c$
n_r	Number of rows of shear connector
n_s	Number of shear connectors in a row
P_s	Tensile force in a shear connector
P_u	Ultimate load of composite box girder
P_{uc}	Capacity of concrete shear cone
r	Resultant stress $r = \sqrt{(\sigma 2c/4)^2 + \tau_c^2}$
T_{bf}	Tensile force in bottom flange in width, w_{e2}
T_{tf}	Tensile force in top steel flange
T_{s1}, T_{s2}	Tensile force in longitudinal reinforcing bars
T_w	Tensile force in web
t_s'	Thickness or distance
t_{bf}, t_{tf}	Thickness of bottom and top steel flange, respectively
t_c	Thickness of concrete deck
$\bar{t}_{ec}$	Distance from mid-thickness of top steel flange to elastic centroid of combined compression flange
$\bar{t}_{pc}$	Distance from mid-thickness of top steel flange to plastic centroid of combined compression flange
t_w	Thickness of web
V_{cr}	Buckling strength of one web panel
V_t	Tension field strength of one web panel

V_u	Ultimate strength of one web panel
v_s	Notations of volume for simplifying computations
w_{e1}	Half of the equivalent width of concrete deck of box girder
w_{e2}	Half of the equivalent width of bottom steel flange of box section
y_{bf}, y_{tf}	Centroidal distance to mid-thickness of bottom and top steel flange, respectively, of equivalent box section
z_1	Distance from left support to left boundary of panel
α	Coefficient of distance, defining position of load from left support
α_c	$\alpha_c = a/b\ (1 - \frac{C_1 + C_2}{a})$
α_c'	$\alpha_c' = a/b\ (1 - \frac{C_2}{a})$
β_1	Coefficient for height of equivalent rectangular concrete stress block
δ	Angle of resultant stress r
ε_{bf}^{cr}	Strain in steel bottom flange at web buckling
ε_c	Strain in concrete
$\varepsilon_{s1}, \varepsilon_{s2}$	Strain in longitudinal reinforcing bars
ε_{tf}	Strain at mid-thickness of top steel flange
σ_{1c}	Critical compressive stress at top edge of web panel
σ_{2c}	Normal stress at bottom edge of web panel, concurrent to σ_{1c}

NOTATIONS (continued)

σ_{bf}^{c}, σ_{bf}^{i}	Nornal stress in bottom flange concurrent to M_p^c and M_p^i, respectively
σ_{bf}^{cr}	Normal stress in bottom flange at web buckling
σ_{bf}^{y}, σ_{tf}^{y}	Yield stress of bottom and top steel flange, respectively
σ_{s1},σ_{s2}	Stress in longitudinal reinforcing bars in top and bottom layer, respectively
σ_{s1}^{y}, $_{s2}^{y}$	Yield stress of longitudinal reinforcing bars
σ_t	Tension field stress
σ_{tf}	Stress in top steel flange
σ_{yw}	Yield stress of web
σ^u	Ultimate tensile strength of steel
τ	Shearing stress
τ_c	Shearing stress in web panel, concurrent to σ_{lc}
ϕ	Tension field angle
ϕ_{ao}	Approximate optimal tension field angle
ϕ_o	Optional tension field angle

REFERENCES

1. Corrado, J. A.
   ULTIMATE STRENGTH OF SINGLE-SPAN RECTANGULAR STEEL BOX GIRDERS, Ph.D. Dissertation, Lehigh University, Bethlehem, Pa., September 1971.

2. Corrado, J. A. and Yen, B. T.
   FAILURE TESTS OF RECTANGULAR MODEL STEEL BOX GIRDERS, Journal of the Structural Division, ASCE, Vol. 99, No. ST7, July 1973.

3. Yen, B. T. and Chen, Y. S.
   TESTING OF LARGE-SIZE COMPOSITE BOX GIRDERS, Fritz Engineering Laboratory Report No. 380.11, Lehigh University, Bethlehem, Pa., June 1980.

4. Yen, B. T., et al
   TESTS ON MODEL COMPOSITE BOX GIRDERS (D1 AND D2), Fritz Engineering Laboratory Report No. 380.6, Department of Civil Engineering, Lehigh University, October 1973.

5. Basler, K.
   STRENGTH OF PLATE GIRDERS IN SHEAR, Journal of the Structural Division, Proc. of the ASCE, Vol. 87, ST7, October 1961.

6. Rockey, K. C.
   FACTORS INFLUENCING ULTIMATE BEHAVIOR OF PLATE GIRDERS, Conference on Steel Bridges, June 24-30, 1968. British Constructional Steelwork Association, Institute of Civil Engineers, London.

7. Rockey, K. C. and Skaloud, M.
   INFLUENCE OF FLANGE STIFFNESS UPON THE LOAD CARRYING CAPACITY OF WEBS IN SHEAR, Final Report, IABSE 8th Congress, New York, New York, 1968.

8. Rockey, K. C. and Skaloud, M.
   THE ULTIMATE LOAD BEHAVIOR OF PLATE GIRDERS LOADED IN SHEAR, The Structural Engineer, Vol. 50, No. 1, January 1972.

9. Fujii, T.
   ON AN IMPROVED THEORY FOR DR. BASLER'S THEORY, Final Report IABSE 8th Congress, New York, New York, 1968.

10. Fujii, T., Kukumoto, Y., Nishino, F. and Okumura, T.
RESEARCH WORK ON ULTIMATE STRENGTH OF PLATE GIRDERS AND JAPANESE PROVISIONS ON PLATE GIRDER DESIGN, IABSE Colloquium on Design of Plate and Box Girders for Ultimate Strength, London, 1971.

11. Chern, C. and Ostapenko, A.
ULTIMATE STRENGTH OF PLATE GIRDERS UNDER SHEAR, Fritz Engineering Laboratory Report No. 328.7, Department of Civil Engineering, Lehigh University, August 1969.

12. Komatsu, S.
ULTIMATE STRENGTH OF STIFFENED PLATE GIRDERS SUBJECTED TO SHEAR, IABSE Colloquium on Design of Plate and Box Girders for Ultimate Strength, London, 1971.

13. Porter, D. M., Rockey, K. C. and Evans, H. R.
THE COLLAPSE BEHAVIOR OF PLATE GIRDERS LOADED IN SHEAR, The Structural Engineer, Vol. 53, No. 8, August 1975.

14. Basler, K.
STRENGTH OF PLATE GIRDERS UNDER COMBINED BENDING AND SHEAR, Journal of the Structural Division, Proc. of the ASCE, Vol. 87, ST7, October 1961.

15. Akita, Y. and Fujii, T.
ON ULTIMATE STRENGTH OF PLATE GIRDERS, Japan Shipbuilding and Marine Engineering, Vol. 3, No. 3, May 1968.

16. Chern, C. and Ostapenko, A.
UNSYMMETRICAL PLATE GIRDERS UNDER SHEAR AND MOMENT, Fritz Engineering Laboratory Report No. 328.9, Department of Civil Engineering, Lehigh University, Bethlehem, Pa., October 1970.

17. Chen, Y. S. and Yen, B. T.
ANALYSIS OF COMPOSITE BOX GIRDERS, Fritz Engineering Laboratory Report No. 380.12, Lehigh University, Bethlehem, Pa., March 1980.

18. Selberg, A.
ON THE SHEAR CAPACITY OF GIRDER WEBS, IABSE Publications, Vol. 34-I, 1974.

19. Joint Committee of the Welding Research Council and the ASCE
PLASTIC DESIGN IN STEEL, A GUIDE AND COMMENTARY, ASCE, 1971.

20. Winter, G. and Nilson, A. H.
DESIGN OF CONCRETE STRUCTURES, 8th Edition, McGraw Hill Book Company, Inc., New York, New York, 1972.

21. ACI Committee 318
BUILDING CODE REQUIREMENTS FOR REINFORCED CONCRETE, American Concrete Institute, Detroit, Michigan, 1971.

22. AASHTO
STANDARD SPECIFICATIONS FOR HIGHWAY BRIDGES, The American Association of State Highway and Transportation Officials, 16th Edition, Washington, D. C., 1979.

23. AISI
SPECIFICATION FOR THE DESIGN OF COLD-FORMED STEEL STRUCTURAL MEMBERS, American Iron and Steel Institute, New York, New York, 1968.

24. Johnston, B. G. (Editor)
GUIDE TO STABILITY DESIGN CRITERIA FOR METAL STRUCTURES, 3rd Edition, John Wiley & Sons, New York, New York, 1976.

25. The Column Research Committee of Japan
HANDBOOK OF STRUCTURAL STABILITY, Corona Publishing Company, Tokyo, Japan, 1971.

26. Nelson Division
EMBEDMENT PROPERTIES OF HEADED STUDS, Nelson Division, TRW Inc., Lorain, Ohio, 1974.

27. Chen, Y. S.
ULTIMATE STRENGTH OF RECTANGULAR COMPOSITE BOX GIRDERS, Ph.D. Dissertation, Lehigh University, Bethlehem, Pa., December 1976.